THE DEMOCRATIC REPUBLIC OF ALGERIA
UNIVERSITY OF SAAD DAHLEB - BLIDA 1 -
INSTITUTE OF AERONAUTICS AND SPACE STUDIES

A dissertation

Submitted in partial fulfilment for the enquiry of an

ACADEMIC MASTER's

In Aeronautics Engineering
Navigation Department

Major : CNS / ATM
Communication Navigation Surveillance / Air trafic Management

THEME

ADAPTIVE CLMDK-CFAR AND OS-CFAR INTERFERENCE-CENSORING DETECTORS IN FUSION BASED ON GENETIC ALGORITHM

Realised by: AISSOUG Asma

Advisor: Dr. DOUDOU Faiza Fatma Zahra

Blida, June 2024

Abstract

This thesis investigates adaptive detection techniques using CA-OS and CMLDK-CFAR sensors for threshold optimization. The focus is on improving the performance of these sensors in varying environments by employing genetic algorithms (GAs). By adjusting thresholds adaptively, the proposed method enhances detection accuracy, providing a robust solution to optimize sensor performance in complex systems.

Key words

CA-CFAR, OS-CFAR, CMLDK-CFAR, GA's, ADAPTIVE DETECTION.

Résumé

Cette thèse explore les techniques de détection adaptatives en utilisant les capteurs CA-OS et CMLDK-CFAR pour l'optimisation des seuils. L'accent est mis sur l'amélioration des performances de ces capteurs dans des environnements variés en employant des algorithmes génétiques (AG). En ajustant les seuils de manière adaptative, la méthode proposée améliore la précision de détection, offrant une solution robuste pour optimiser les performances des capteurs dans des systèmes complexes.

Mots-clés

CA-CFAR, OS-CFAR, CMLDK-CFAR, AG, DÉTECTION ADAPTATIVE

Acknowledgments

I would like to extend my deepest gratitude and appreciation to my thesis advisor, Dr. Doudou Faiza Fatma Zahra, for her exceptional guidance throughout this research. Her dedication from the very beginning of this project, her patience, and the invaluable opportunity she provided to delve into the world of algorithms have been truly instrumental. I also wish to express my sincere thanks to the reviewers of my thesis for their insightful comments and feedback.

I would also like to thank my Mom and Dad, my two sisters Yeya and Mina whom I love so much and my little brother zinou.
To my two most precious friends Maroua Hadj Said and Feriel Zekri whom I cherish the most.

To the administration staff and the class of CNS/ATM 2024, I thank you all.

Contents

Abstract .....

Acknowledgments.....

Symbols.....

Acronyms.....

List of figures .....

List of tables.....

Preface.....

1 Introduction to Radar Systems and Signal Processing.....13

1.1 History and Applications of Radar.....13

1.2 Radar System Classification 14

1.3 Clutter And Noise.....14

1.3.1 Definition of Noise 15

1.3.2 Definition of Clutter.....15

1.4 Basic Radar Functions 15

1.5 The Doppler Shift.....17

1.6 Elements of a Pulsed Radar 17

1.6.1 Transmitter and Waveform Generator 18

1.6.2 Antennas 20

1.6.3 Receivers.....21

1.6.4 Resolution 23

1.7 Radar equation 24

1.7.1 Tracking.....26

1.7.2 Volume search 26

1.7.3 Clutter.....26

1.8 Range Ambiguity 27

1.9 Fluctuating target models 28

1.9.1 Swerling model 1.....29

1.9.2 Swerling model 2.....29

1.9.3 Swerling model 3.....29

1.9.4 Swerling model 4.....30

1.9.5 Swerling model 5 (or 0) 30

1.10 Signal processing phase....31
2 Detection fundamentals....37
2.1 Radar Detection as Hypothesis Testing....37
2.2 The Neyman-Pearson Detection Rule....38
2.3 The Likelihood Ratio Test....39
2.4 Bayes' criterion....42
2.5 Parameter Estimation....43
2.5.1 Maximum Likelihood Estimation....43
2.6 Detection techniques....45
2.6.1 Optimal detection....47
2.6.2 Fixed Threshold Detection....48
2.6.3 Adaptive Threshold Detection....49
3 Adaptive thresholding CFAR Detection....52
3.1 Introduction....52
3.2 Environment (background)....53
3.2.1 Homogenous background....54
3.2.2 non homogenous background....54
3.3 Adaptive CFAR Detection....55
3.3.1 principles....55
3.3.2 Cell Averaging CFAR Detection....57
3.3.3 Order Statistic CFAR....61
3.3.4 CMLD-K CFAR....62
4 Optimization using Evolutionary Algorithms....65
4.1 introduction (Evolutionary Algorithms)....65
4.2 Genetic Algorithm....67
4.2.1 Introduction....67
4.2.2 Background....68
4.2.3 Natural selection....68
4.2.4 Genetic algorithm vocabulary....69
4.2.5 Encoding and Representation....69
4.2.6 Selection Mechanisms in Genetic Algorithms....71
4.2.7 Basic Principle....73
4.3 Simulation description....76
4.4 OS-CFAR threshold optimization in distributed systems....79
4.5 CMLD-CFAR threshold optimization in distributed systems....80
5 References....89

List of figures

Figure 1.1Basic principle of radar 16
Figure 1.2 Spherical coordinate system for radar measurements. 16
Figure 1.3 Block diagram of a pulsed monostatic radar. 18
Figure 1.4 One-way atmospheric attenuation of electromagnetic waves. 19
Figure 1.5 Effect of different rates of precipitation on one-way atmospheric attenuation of electromagnetic waves 20
Figure 1.6 Examples of typical array and aperture antennas. (a) Slotted phased array in the nose of an F/A-18 aircraft. This antenna is part of the AN/APG-73 radar system. (b) A Cassegrain reflector antenna 20
Figure 1.7 Conventional quadrature channel receiver model. In this illustration, the lower channel is the in-phase ("I") channel, and the upper is the quadrature phase ("Q") channel. 21
Figure 1.8 (a) The I channel of the receiver in Fig. 1.6 measures only the cosine of the phasor θ(t). (b) The Q channel measures only the sine of the phasor. 22
Figure 1.9 Structure of a superheterodyne radar receiver. 22
Figure 1.10 Geometry for describing conventional pulse range resolution 23
Figure 1.11 The angular resolution is determined by the 3-dB antenna 24
Figure 1.12 Swerling 1 29
Figure 1.13 Swerling 2 29
Figure 1.14 Swerling 3 30
Figure 1.15 Swerling 4 30
Figure 1.16 Swerling 5 31
Figure 1.17 Signal and data processing in a modern pulse radar system. 32
2.1 detection principle Figure 45
Figure 2.2 A Radar Scan 46
Figure 2.3 Diagram of a Conventional Detector 47
Figure 2.4 Principle of fixed threshold detection 49
Figure 2.5 Principle of adaptive threshold detection 50
Figure 3.1 Effect of the noise power increase on the probability of false alarm for a fixed threshold; design Pfa =10−6 53
Figure 3.2 reference window scans a homogenous and non-homogenous environment 54
Figure 3.3 different situations of non-homogenous environnement 55
*Figure 3.4 A scheme for a fixed threshold radar detection 56
Figure 3.5 Optimum receiver, square realization. 56
Figure 3.6 A scheme for an adaptive threshold radar detection. 56
Figure 3.7 Range and Doppler sampling process 57
Figure 3.8 Matrix of range and Doppler cells. 58
Figure 3.9 Cell averaging CFAR detector. 58
Figure 3.10 OS-CFAR Detector 61
Figure 3.11 CML-CFAR Detector 62
Figure 4.1 Timeline of various EAs 66
Figure 4.2 A roulette-wheel marked for five individuals according to their fitness values. Third individual has a higher probability of selection than any other 72
Figure 4.3 The Working Principle of a Simple Genetic Algorithm 73

Figure 4.4 The basic GA operations: One generation is broken down into a selection phase and recombination phase. Strings are assigned into adjacent slots during selection. 74
Figure 4.5 Probability of Detection using OR Fusion Rule with OS_CFAR in Different Backgrounds 83
Figure 4.6 Probability of Detection using AND Fusion Rule with OS_CFAR in Different Backgrounds 84
Figure 4.7 Probability of Detection using OR Fusion Rule with CMLD_CFAR in Different Backgrounds 84
Figure 4.8 Probability of Detection using AND Fusion Rule with CMLD_CFAR in Different Backgrounds 85
Figure 4.9 Probability of Detection using OR Fusion Rule with CMLD_CFAR for Different Sensor Systems 87

List of tables

Table 1-1 Letter Nomenclature for Nominal Radar Frequency Bands 19
Table 2-1 Decision Hypothesis 48
Table 4-1 Genetic Algorithm Terms 69
Table 4-2 OS-CFAR using GAs (with OR fusion rule) 79
Table 4-3 OS-CFAR using GAs (with AND fusion rule) 79
Table 4-4 CMLD-CFAR using GAs (with OR fusion rule) 80
Table 4-5 CMLD-CFAR using GAs (with AND fusion rule) 80
Table 4-6 Detection Probability Comparison for CMLD and OS-CFAR Methods Across Various SNR Levels and Fusion Rules 86

Symbols

dB Decibel

b Noise

c speed of light

H0 The hypothesis of only noise existence

H1 The hypothesis of noise plus signal existence

PDF probability density function

PD probability of detection

Pfa probability of false alarm

Z CFAR noise estimator

S signal – to - noise ratio

N Number of reference cells

U,V Half of reference window

α0 overall desired probability of false alarm

Acronyms

CFAR constant false alarm

CA-CFAR cell averaging CFAR

OS-CFAR order statistic CFAR

CMLDk-CFAR censoring mean level detector CFAR

T-CA CA-CFAR scaling factor

T-OS OS-CFAR scaling factor

T-CMLD CMLDk-CFAR scaling factor

CUT cell under test

GA genetic algorithm

General introduction

Radar systems play a vital role in detecting and tracking targets across different environments, whether they are uniform or vary significantly. One of the key objectives in radar signal processing is to achieve high detection accuracy while keeping the false alarm rate consistent. However, conventional CFAR detectors often struggle in non-uniform environments, where noise and clutter levels fluctuate. This challenge highlights the need for more advanced CFAR methods that can adapt to dynamic conditions and ensure reliable target detection.

This thesis focuses on enhancing the performance of **Constant False Alarm Rate (CFAR)** systems through the use of **Genetic Algorithms (GAs)**. CFAR detectors, particularly **OS-CFAR** and **CMLD-CFAR**, play a critical role in radar systems by detecting targets while maintaining a constant false alarm rate despite varying environmental conditions. The primary challenge is to improve the **probability of detection (Pd)** without increasing the **probability of false alarms (Pfa)**, especially in non-homogeneous environments. This study leverages GAs, an evolutionary algorithm, to optimize key CFAR parameters such as **rank order (K)** and **threshold (T)** values to overcome the limitations of traditional CFAR detectors.

GAs are particularly well-suited for this optimization task due to their ability to explore a large solution space and avoid local optima, which can hinder detection performance. The GA process in this study involves initializing a population of solutions, applying crossover and mutation operations to create offspring, and using selection strategies like **Tournament Selection** to guide the population toward the best solutions. Through this iterative process, the CFAR systems can dynamically adjust to changing conditions and interference, leading to better performance across a range of Signal-to-Noise Ratios (SNRs) and background conditions.

Chapter 1:

provides a theoretical fundament introduction to radar concepts as well as its functionality principles.

Chapter 2:

explains the concept of Radar detection and its types of thresholding methods

Chapter 3:

gives an overview of CFAR detectors and their probabilistic studies

Chapter 4:

introduction to evolutionary algorithms including GA's (backgound, encoding representation and other important parameters)

Simulation and representation:

the results of the simulations are presented and analysed. The performance of OS-CFAR and CMLD-CFAR detectors optimized by GAs is compared under various SNR levels and background conditions

CHAPTER 01

Introduction to Radar Systems and Signal Processing

SUMMARY

This chapter introduces a brief history of the radar system, its components, its operating principle, and a citation of different types, including a definition of clutter and noise. In addition, we talk about the radar equation, the Swerling fluctuating target models, the Doppler Effect, and then we quote generally the parts of the radar signal processing knowing that our project aims at a part of this processing.

1 Introduction to Radar Systems and Signal Processing

1.1 History and Applications of Radar

The term "radar" originated from the acronym RADAR, meaning "radio detection and ranging." It has been used in various applications since its inception, including measuring speed limits, enforcing speed limits, and detecting aircraft. The development of radar accelerated in the mid-1930s, with independent developments in the United States, Britain, France, Germany, Russia, Italy, and Japan.

In the United States, R. M. Page of NRL began developing pulsed radar in 1934, leading to the development of the SCR-268 antiaircraft fire control system and the SCR-270 early warning system. British development began in 1935 with work by Watson-Watt, demonstrating pulsed radar and establishing the Chain Home surveillance radar network. By the end of World War II, the value of radar and the advantages of microwave frequencies and pulsed waveforms were widely recognized.

The military is still a major user and developer of radar technology, with applications spanning from large ballistic missile defence systems to fist-sized tactical missile seekers. Radar now enjoys an increasing range of applications, including police traffic radar, colour weather radar, air traffic control systems, aviation, collision avoidance and buoy detection by ships, automobile and trucking industries, and spaceborne and airborne radar.

This text aims to present a thorough, straightforward, and consistent description of the signal processing aspects of radar technology, focusing on the more fundamental functions common to most radar systems. Pulsed radars are emphasized over CW radars, while monostatic radars are emphasized over bistatic radars. The subject is approached from a digital signal processing (DSP) viewpoint as much as practicable, as most new radar designs rely heavily on digital processing and can unify concepts and results often treated separately [1].

1.2 Radar System Classification

➢ Based on target's type

- Secondary RADAR

Radars known as secondary radars depend on a target response for their operation. Most of these devices are used for navigation and telecommunications.

- Primary RADAR

Primary radars can be of the two-dimensional type giving range and azimuth measurements or of the three-dimensional type, for which an additional elevation angle measurement is then available. There are primary approach radars which are located at airports and are intended to detect all aircraft approaching an airport.

➢ Based on the relative position of transmitter or the receiver

- Monostatic: reception and transmission are done with the same antenna.
- Multi-static: two antennas or plus for reception and transmission separated with a certain distance.

➢ Based on the signal's type

- Pulse Radar

Conventional pulse radar emits rectangular pulses of unmodulated duration. However, a new technique is used to modulate the frequency to obtain an ideal receiver.

- Continious wave RADAR (CW RADAR)

In this type of radar, the transmitter generates a continuous oscillation at frequency f0 which is radiated by the antenna. A portion of the transmitted signal is reflected by the target and is intercepted by the antenna. The frequency of the received signal will be shifted from that of the transmitted signal f0 by an amount ± fd which is the Doppler frequency. A Doppler amplifier is used to eliminate echoes from stationary targets and to amplify the signal to make it usable.

➢ Based on objectif

- Surveillance: Radar explores continuously the coverage area.
- Tacking: Radar tracks a target continuously or discontinuously (track while scan)[4].

1.3 Clutter And Noise

- In modern tracking and surveillance radar, the declaration of the presence or absence of a target is made based on a comparison of the received echo signal against a predefined threshold. This signal is generated from three different sources[7],

- From the target.
- Thermal noise.
- The surrounding clutter.

1.3.1 Definition of Noise

In reality the signal processed by the detector to decide is always accompanied by background noise of a random nature.
This background noise is made up of two types of noise: the first, present in all physical devices, is the result of interference from signals from different sources such as thermal noise in absolute temperature systems. The second type of noise is called clutter.

1.3.2 Definition of Clutter

Clutter refers to echoes produced by unwanted targets such as the ground, sea, rain, etc. It results from an aggregation of echoes from small but numerous reflectors, such as raindrops, sea waves, swarming insects. The definition of clutter depends on the type of targets the radar is looking for. If a radar considers aircraft to be useful targets, then rain is clutter to it; a weather radar, on the other hand, considers rain to be a useful target and aircraft to be clutter.
If a target's echo is drowned in clutter, the radar may miss its detection as it may give a series of false alarms by considering the clutter as a set of targets. Detection in a clutter environment is a primary problem for modern radar and continues to be a subject of research as existing detectors are not suitable for all situations.

1.4 Basic Radar Functions

Most uses of radar can be classified as *detection, tracking*, or *imaging*. This text addresses all three, as well as the techniques of signal acquisition and interference reduction necessary to perform these tasks. The most fundamental problem in radar is detection of an object or physical phenomenon. This requires determining whether the receiver output at a given time represents the echo from a reflecting object or only noise. Detection decisions are usually made by comparing the amplitude $A(t)$ of the receiver output (where t represents time) to a threshold $T(t)$, which may be set a priori in the radar design or may be computed adaptively from the radar data;
The time required for a pulse to propagate a distance R and return, thus traveling a total distance 2R, is just 2R/c; thus, if A(t) > T(t) at some time delay t0 after a pulse is transmitted, it is assumed that a target is present at range

$$R = \frac{ct_0}{2} \tag{1.1}$$

where c is the speed of light [1].

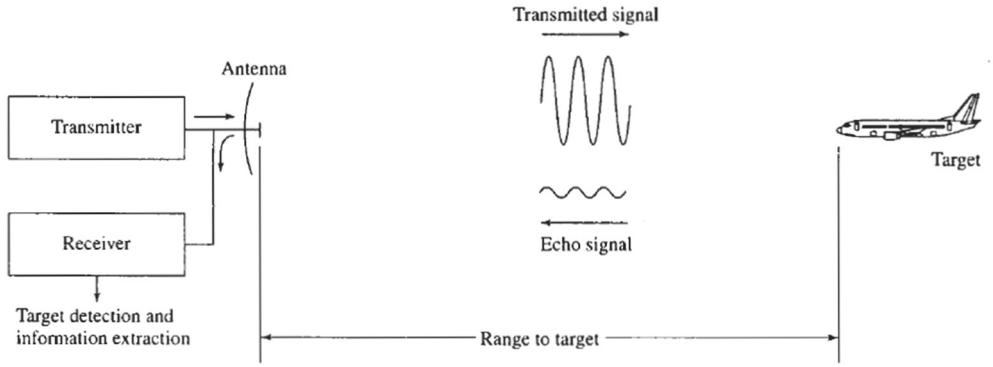

Figure 1.1Basic principle of radar

After detecting an object, radar may need to track its location or velocity. In a monostatic radar system, position is naturally measured in a spherical coordinate system with the radar antenna's phase center as the origin. This coordinate system, illustrated in Fig. 1.1, has the antenna's look direction aligned with the positive x-axis. The angles θ and ϕ represent azimuth and elevation, respectively. The range to the object is directly calculated from the time taken for the radar pulse to travel to the object and back. Elevation and azimuth angles are determined based on the antenna's orientation, as the target typically needs to be within the antenna's main beam for detection. Velocity estimation involves measuring the Doppler shift of the target echoes. While Doppler shift provides only the radial velocity component, tracking over time allows inference of the target's dynamics in all three dimensions [1].

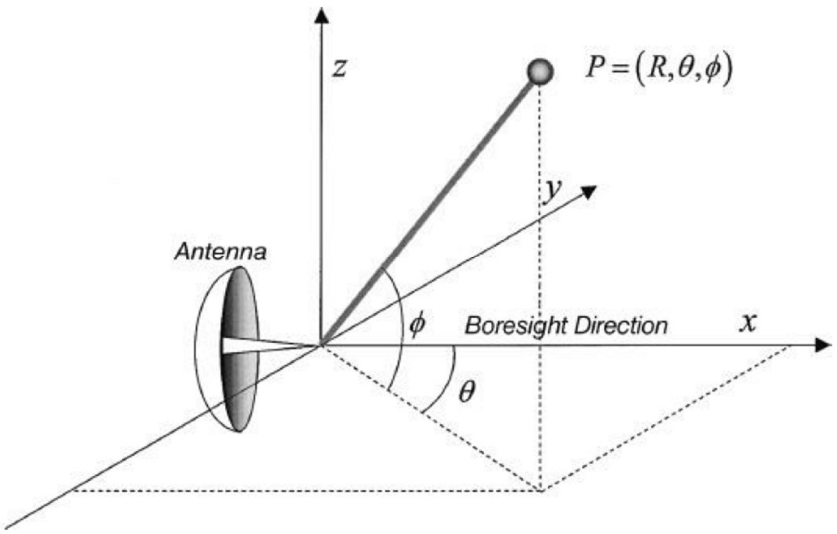

Figure 1.2 Spherical coordinate system for radar measurements.

1.5 The Doppler Shift

An accurate way of measuring the speed of a target is the use of *Doppler frequency* shift, which is the difference between the received frequency and the transmitted frequency caused by the motion of the target. In this case, a *coherent* system is needed, in the sense that the transmitter and the receiver oscillators are phase locked, in order to detect any difference in the echo signal. Thus:

$$f_d = f_r - f_t \tag{1.2}$$

Where f_d is Doppler frequency, *fr* is the receiver frequency, and *ft* is the transmitter frequency. Doppler frequency is given in terms of *vr*, the radial component of the target speed toward the radar, by

$$f_d = \frac{2v_r}{\lambda} \tag{1.3}$$

where $vr << c$, c is the speed of light, and the *wavelength* λ is given by

$$\lambda = \frac{c}{f_t} \tag{1.4}$$

For fixed objects, *fd* equals zero.

1.6 Elements of a Pulsed Radar

Figure 1.2 depicts a basic block diagram of a simple pulsed monostatic radar system. The waveform generator produces the desired pulse waveform, which is then modulated to the desired radio frequency (RF) and amplified for transmission. The transmitted signal is directed to the antenna through a duplexer, which switches between transmit and receive modes. Returning echoes are routed back through the duplexer into the radar receiver. Typically, the receiver employs a superheterodyne design, with an initial stage consisting of a low-noise RF amplifier. Subsequent stages involve modulation of the received signal to successively lower intermediate frequencies (IFs) until reaching baseband, where no carrier frequency modulation occurs. Each modulation step involves a mixer and a local oscillator (LO).The baseband signal then undergoes processing in the signal processor, which performs various functions such as pulse compression, matched filtering, Doppler filtering, integration, and motion compensation. The output of the signal processor varies based on the radar's purpose. For example, a tracking radar provides a stream of detections with measured range and angle coordinates, while an imaging radar produces a two- or three-dimensional image.

Finally, the processed data is sent to the system display, data processor, or both, depending on the specific requirements of the radar system [1].

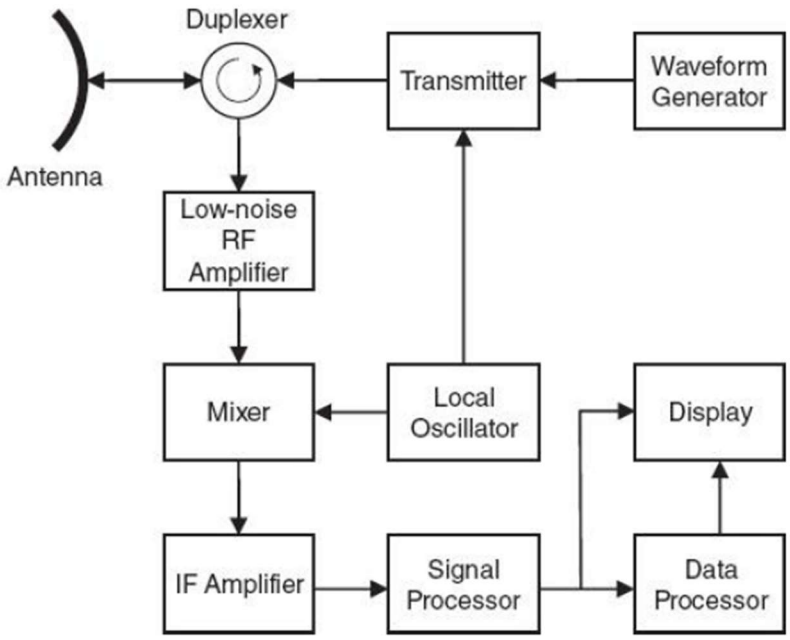

Figure 1.3 Block diagram of a pulsed monostatic radar.

1.6.1 Transmitter and Waveform Generator

The transmitter and waveform generator are critical components that impact the sensitivity and range resolution of radar systems. Radar systems operate across a wide range of frequencies, from as low as 2 MHz to as high as 220 GHz, with laser radars operating at even higher frequencies in the terahertz range. However, the majority of radar systems operate in the microwave frequency range, typically between 200 MHz and 95 GHz, corresponding to wavelengths ranging from 0.67 meters to 3.16 millimeters.

Table 1.1 provides a summary of the letter nomenclature commonly used for different radar bands. Additionally, the millimeter wave band can be further subdivided into sub bands such as the Q band (36 to 46 GHz), V band (46 to 56 GHz), and W band (56 to 100 GHz). These frequency bands and their corresponding wavelengths are essential considerations in radar design and operation [1].

Band	Frequencies	Wavelengths
HF	3–30 MHz	100–10 m
VHF	30–300 MHz	10–1 m
UHF	300 MHz–1 GHz	1–30 cm
L	1–2 GHz	30–15 cm
S	2–4 GHz	15–7.5 cm
C	4–8 GHz	7.5–3.75 cm
X	8–12 GHz	3.75–2.5 cm
K_u	12–18 GHz	2.5–1.67 cm
K	18–27 GHz	1.67–1.11 cm
K_a	27–40 GHz	1.11 cm–7.5 mm
mm	40–300 GHz	7.5–1 mm

Table 1-1 Letter Nomenclature for Nominal Radar Frequency Bands

Figure 1.4 illustrates atmospheric attenuation for one-way propagation over the most common radar frequency ranges under a set of atmospheric conditions. Most Ka-band radars operate near 35 GHz and most W-band systems operate near 95 GHz due to the relatively low atmospheric attenuation at these wavelengths.

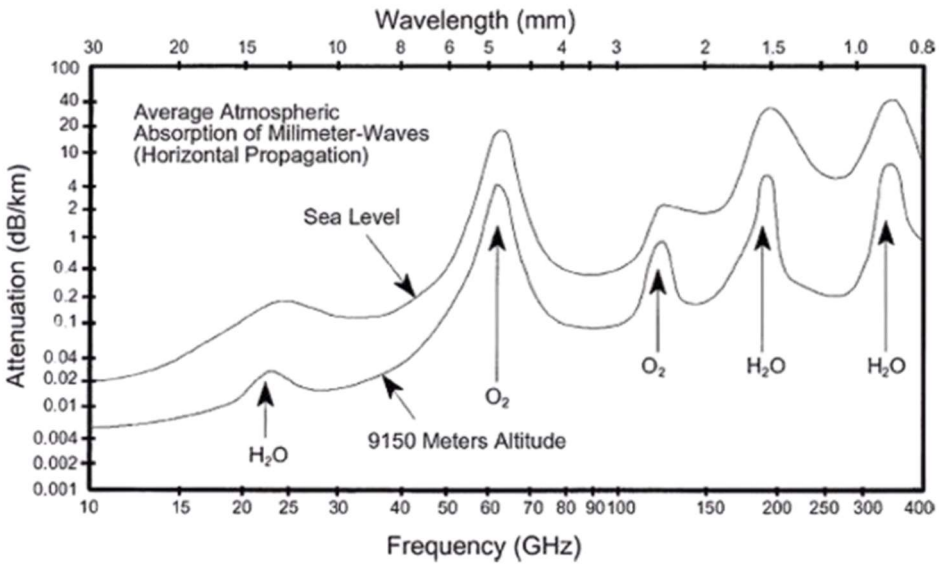

Figure 1.4 One-way atmospheric attenuation of electromagnetic waves.

Weather conditions can also have a significant effect on radar signal propagation. Figure 1.5 illustrates the additional one-way loss as a function of RF frequency for rain rates ranging from drizzle to a tropical downpour.

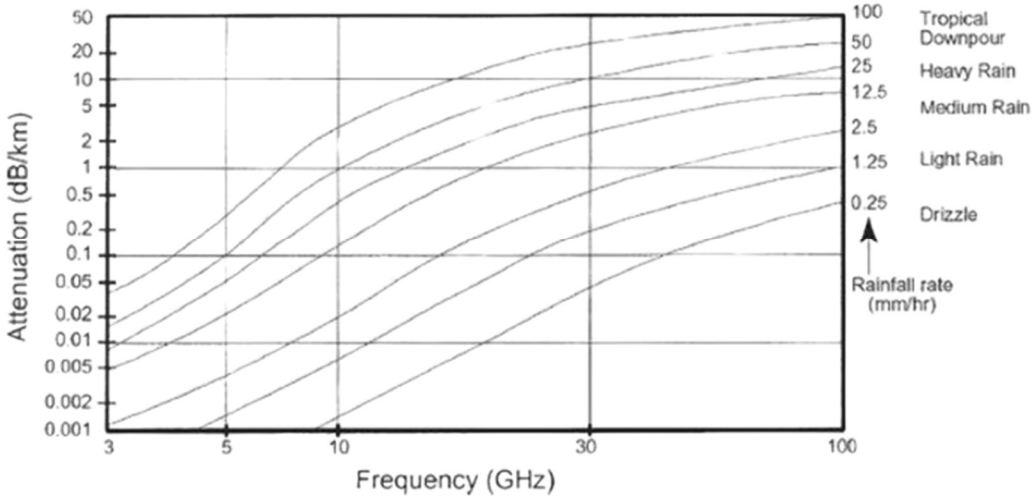

Figure 1.5 Effect of different rates of precipitation on one-way atmospheric attenuation of electromagnetic waves.

1.6.2 Antennas

The antenna plays a major role in determining the sensitivity and angular resolution of the radar. A wide variety of antenna types are used in radar systems. Some of the most common types are parabolic reflector antennas, feed scanning antennas, lens antennas, and phased array antennas.

The radiation pattern follows the line of sight. The gain G and the effective aperture Ae are important. The 3 dB beamwidth of the uniformly illuminated aperture in radians is λ/D, which is inversely proportional to the antenna aperture D and proportional to the wavelength λ [1].

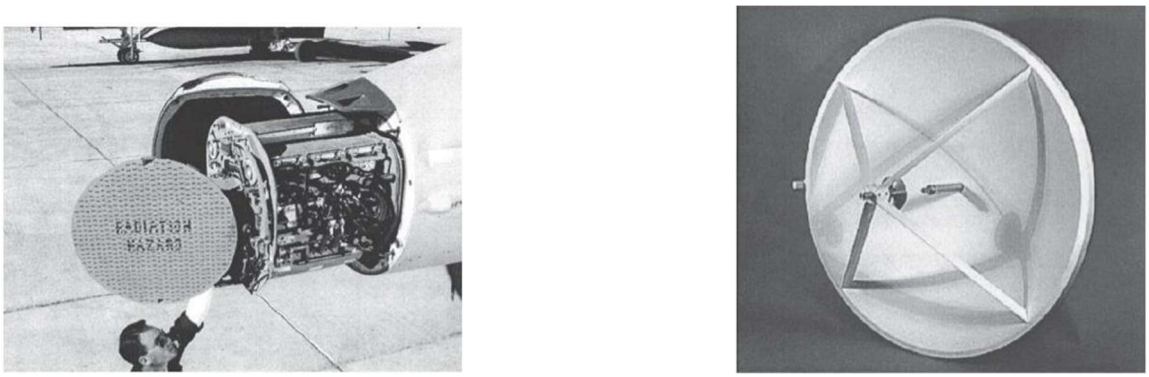

(a) (b)

Figure 1.6 Examples of typical array and aperture antennas. (a) Slotted phased array in the nose of an F/A-18 aircraft. This antenna is part of the AN/APG-73 radar system. (b) A Cassegrain reflector antenna.

1.6.3 Receivers

It has been shown that radar signals are generally narrowband, passband functions with phase or frequency modulation. This means that the received echo waveform r(t) from a single scatterer is of the form:

r(t) = A(t) (sin ωt $+\theta$(t)) where the amplitude modulation A(t) represents only the pulse envelope. The main function of the receiver processing is the demodulation of the information-carrying part of the radar signal to baseband, with the goal of measuring θ(t). Figure 1.6 illustrates the conventional approach to receiver design used in most classical radars.

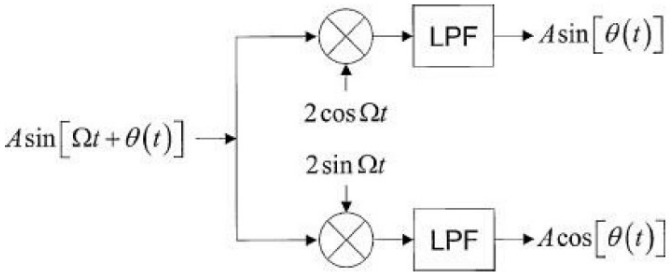

Figure 1.7 Conventional quadrature channel receiver model. In this illustration, the lower channel is the in-phase ("I") channel, and the upper is the quadrature phase ("Q") channel.

The reason why both I and Q channels are necessary is that either one alone does not provide enough information to unambiguously determine the phase modulation θ(t). Figure 1.7 illustrates the problem. Consider the case shown in Fig. 1.7a. The signal phase θ(t) is represented by a solid black phasor in the complex plane. If only the I channel is implemented in the receiver, only the cosine of θ(t) will be measured. In this case, the true phasor will be indistinguishable from the gray phasor - θ(t). Similarly, if only the Q channel is implemented so that only the sine of θ(t) is measured, then the true phasor will be indistinguishable from the gray phasor in Figure 1.7b, which corresponds to π-θ(t). When both I and Q channels are implemented, the quadrant of the phasor is determined unambiguously. In fact, the signal processor will typically assign the I signal to the real part of a complex signal and the Q signal to the imaginary part, forming a single complex signal [1].

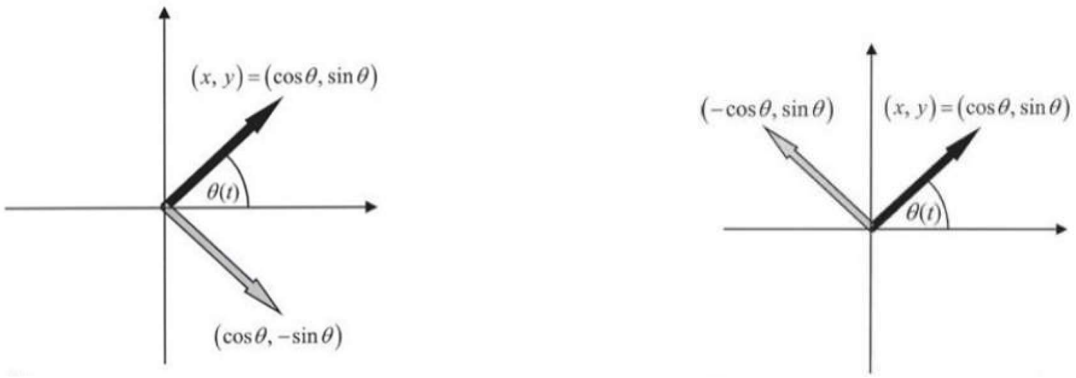

(a) (b)

Figure 1.8 (a) The I channel of the receiver in Fig. 1.6 measures only the cosine of the phasor θ(t). (b) The Q channel measures only the sine of the phasor.

In the receiver structure shown in Figure 1.6, the information-bearing part of the signal is demodulated from the carrier frequency to the baseband in a single mixing operation. While this is convenient for analysis, pulsed radar receivers are practically never implemented this way in practice.

Figure 1.8 shows a more representative superheterodyne receiver structure. The received signal, which is very weak, is immediately amplified upon reception using a low noise amplifier (LNA). The LNA, more than any other component, determines the noise figure of the overall receiver. The key feature of the superheterodyne receiver is that baseband demodulation occurs in two or more stages. First, the signal is modulated to an intermediate frequency (IF), where it receives additional amplification. Amplification at IF is easier due to the higher percentage bandwidth of the signal and the lower cost of IF components compared to microwave components. Finally, the amplified signal is demodulated to the baseband. Some receivers may use more than two stages of demodulation (so there are at least two IF frequencies), but two stages are the most common choice [1].

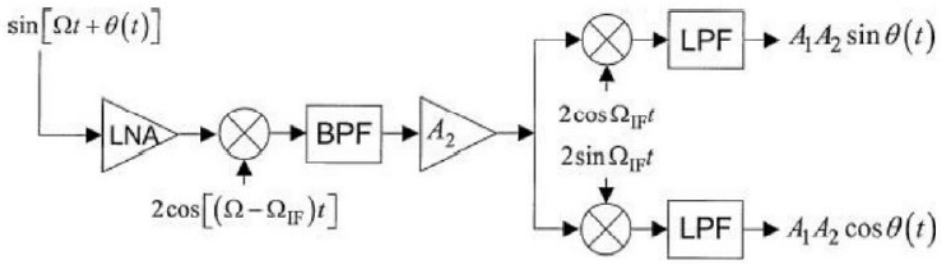

Figure 1.9 Structure of a superheterodyne radar receiver.

1.6.4 Resolution

The closely related concepts of resolution and resolution cell will frequently appear. Two scatterers of equal strength are considered resolved if they produce two separately identifiable signals at the system output, as opposed to combining into a single undifferentiated output. The idea of resolution is applied in range, cross-range, Doppler shift or velocity, and angle of arrival. Two scatterers can be resolved simultaneously in one dimension, say range, and not be resolved in another, perhaps velocity.

The resolution of a radar determines the size of a resolution cell. A resolution cell in range, velocity, or angle is the interval in that dimension that contributes to the echo received by the radar at any given time. Figure 1.9 illustrates resolution and the resolution interval in the radial distance dimension for a simple constant frequency pulse. To resolve the contributions of two scatterers at different time samples, they must be spaced more than cτ/2 meters apart so that their individual echoes do not overlap in time[1].

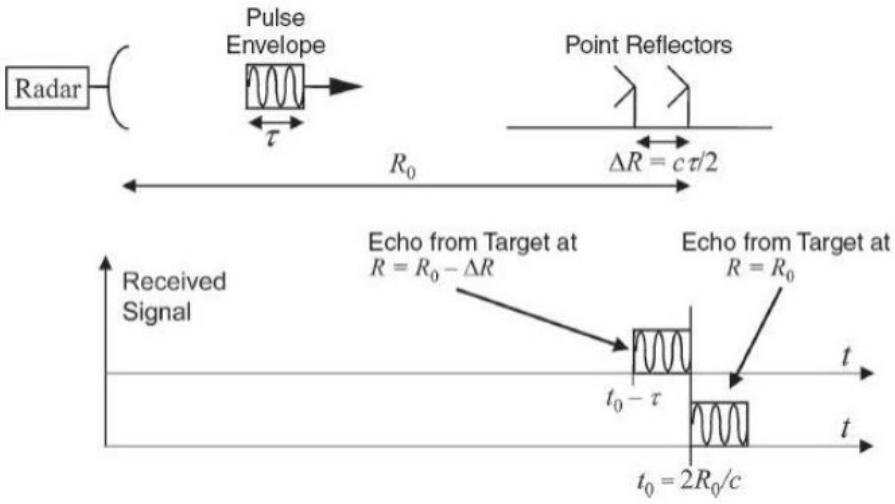

Figure 1.10 Geometry for describing conventional pulse range resolution.

This description of range resolution applies only to unmodulated constant frequency pulses. pulse modulation combined with matched filtering can be used to achieve finer range resolution than cτ/2.

Angular resolution in the azimuthal and elevation dimensions is determined by the antenna beamwidths in the same planes. Thus, the two point scatterers in Figure 1.10 located at the 3 dB edges of the beam define the radar's angular resolution.

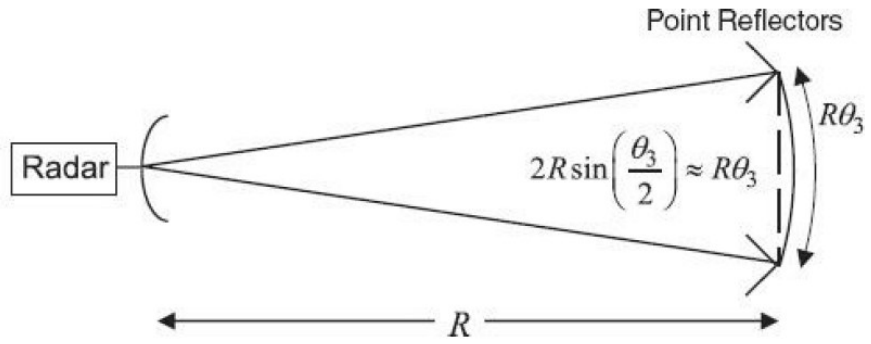

Figure 1.11 The angular resolution is determined by the 3-dB antenna

1.7 Radar equation

The radar equation is crucial for understanding radar performance, as it relates the received signal power Pr to radar characteristics.

$$P_r = \frac{P_t G_t}{4\pi R^2} \times \frac{\sigma}{4\pi R^2} \times A_e \tag{1.2}$$

This equation can be broken down into three main factors. The first factor is the power density at a distance R from a radar transmitting Pt watts with an antenna gain Gt. The second factor involves the target's cross section σ, accounting for the divergence of the electromagnetic wave on its outward and return paths. Together, these two factors represent the power per square meter returned to the radar. The third factor, involving the antenna's effective aperture area Ae, indicates the portion of this returned power intercepted by the radar. The maximum radar range Rmax is determined when the received power Pr equals the receiver's minimum detectable signal Smin, leading to the radar equation.

$$R_{max}^4 = \frac{P_t G_t A_e \sigma}{(4\pi)^2 S_{min}} \tag{1.3}$$

When the same antenna is used for both transmitting and receiving, the transmitting gain Gt and the effective receiving aperture Ae are connected by the relationship$G_t = \frac{4\pi A_e}{\lambda^2}$, where λ is the radar wavelength. By substituting this relationship into the radar equation, we obtain two alternative forms of the equation.

$$R_{max}^4 = \frac{P_t G_t \lambda^2 \sigma}{(4\pi)^3 S_{min}} \tag{1.4}$$

$$R_{max}^4 = \frac{P_t {A_e}^2 \sigma}{4\pi\lambda^2 S_{min}} \tag{1.5}$$

The simplified radar equation examples provided are useful for rough range calculations but are overly optimistic and not realistic. Two main reasons for this inaccuracy are the omission of various radar losses and the statistical nature of the

target cross section and minimum detectable signal. these issues will be addressed later on by refining the radar equation for more accurate range predictions. Although range appears as the fourth power in the equation, it can vary in specific situations. The radar equation is also valuable for preliminary system design by illustrating trade-offs among radar performance parameters.

The minimum detectable signal Smin in the radar equation is a statistical measure that must account for the probability of detection and false alarms. For reliable detection, the signal must exceed noise by 10 to 20 dB at the detection point in the receiver. This minimum detectable signal can be expressed as the signal-to-noise ratio (SNR) required for reliable detection, multiplied by the receiver noise. The receiver noise is the thermal noise, kTB, where k is Boltzmann's constant, T is the temperature, and B is the receiver bandwidth. This noise is then multiplied by the receiver noise figure Fn. The receiver noise figure is measured relative to a reference temperature T0 = 290 K, with kT0 approximating 4×10^{-21}W/Hz. The minimum detectable signal in the radar equation is thus defined.

$$S_{min} = KT_0F_n\frac{S}{N} \tag{1.6}$$

Sometimes, the term T_0F_n is replaced with Js, the system noise temperature. While the radar equation is often discussed in terms of signal power, total signal energy is often more convenient for detecting more complex waveforms. The energy-to-noise ratio E/N0 is a fundamental parameter in statistical detection theory, more so than the signal-to-noise (power) ratio. For a matched filter, the peak signal-to-noise ratio at the output is $2E/N_0$.

For a rectangular pulse of width T, where signal power is E/T and noise power is N_0B (with E as signal energy, N_0as noise energy, or noise power per unit bandwidth, and B as receiver bandwidth), the minimum detectable signal Smin becomes Js(E/N_0)T. Substituting this into the radar equation adjusts the calculation accordingly.

$$R_{max}^4 = \frac{E_tG_tA_e\sigma}{(4\pi)^2KT_0F_n(\frac{E}{N_0})} \tag{1.7}$$

Equation (1.7) applies to a rectangular pulse but can be used for any waveform if Et is the energy in the transmitted waveform and the receiver with noise figure Fn is designed as a matched filter. Some radar detection theory results present the probability of detection and false alarm in terms of S/N rather than E/N_0. For optimal matched-filter processing, the required E/N_0values for the radar equation can be derived from these results for S/N or the visibility factor. The radar equation can be adapted into different forms for specific applications, with several examples provided[7].

1.7.1 Tracking

In this situation the radar is assumed to track continuously or "searchlight" a target for an interval of time t_0. Equation (1.7) applies, so that the 'tracking', or 'searchlighting', radar equation is

$$R_{max}^4 = \frac{P_{av} t_0 G_t A_e \sigma}{4\pi K T_0 F_n (\frac{E}{N_0})} \tag{1.8}$$

Where $P_{av}t_0$= *Et.* Thus, in a tracking radar that must "see" to a long range, the average power must be high, the time on target must be long, and the antenna must be of large electrical size (G,) and large physical size *(Ae).* The frequency does not enter explicitly. Since it is easier mechanically to move a small antenna than a large one, tracking radars are usually found at the higher frequencies, where small apertures can have high gain and thus an adequate G, *Ae* product. The radar equation is based on detectability. A tracking radar must also be designed for good angular accuracy. Good angle accuracy is achieved with narrow beamwidths (large G,) and with high *E/N0* (large *Ae).* Thus, a large *Gt Ae* product is consistent with good tracking accuracy as well as good detectability [4].

1.7.2 Volume search

Assume that the radar must search an angular volume of Ω steradians in the time *ts*. If the antenna beam subtends an angle of Ω_b steradians, the antenna gain G_t, is approximately $4\pi/\Omega_b$. If the antenna beam dwells a time t_0 in each direction subtended by the beam, the total scan time is $ts = t_0\Omega/\Omega_b$ Substituting these expressions into Eq. (1.7) and noting that $\boldsymbol{Et}=P_{av}t_0$

$$R_{max}^4 = \frac{P_{av} A_e \sigma}{4\pi K T_0 F_n (\frac{E}{N_0})} \frac{1}{ts} \tag{1.9}$$

Thus, for a volume search radar the two important parameters for maximizing range are the average transmitter power and the antenna aperture. Any decrease in time to scan the volume or any increase in the volume searched must be accompanied by a corresponding increase in the product $P_{av}A_e$. Note that the frequency does not enter explicitly [4].

1.7.3 Clutter

When a radar must detect a small target on the surface of the sea or land, unwanted clutter echoes can significantly hinder target detectability. When clutter power exceeds receiver noise power, the radar range equation simplifies to an expression for the signal-to-clutter ratio. This ratio equals the target cross-section to clutter

cross-section ratio. If clutter is uniformly distributed, the clutter echo depends on the area illuminated by the radar's resolution cell. Surface clutter (ground or sea) is described by the clutter echo's ratio to the illuminated area, represented by the normalized clutter coefficient σ_0. For a pulse radar viewing the target and clutter at low grazing angles and assuming single-pulse detection, the signal-to-clutter ratio is considered.

$$\frac{S}{C} = \frac{\sigma}{\sigma_0 R \theta_b \left(\frac{c\tau}{2}\right) sec\phi} \tag{1.10}$$

$$R_{max} = \frac{\sigma}{\left(\frac{S}{C}\right)_{min} \sigma_0 \theta_b \left(\frac{c\tau}{2}\right) sec\phi} \tag{1.11}$$

where R = range to clutter patch

θ_b = azimuth beamwidth

c = velocity of propagation

τ = pulse width

ϕ = grazing angle

The clutter patch is determined by the antenna beam width in azimuth and by the pulse width in the range coordinate. The signal-to-clutter ratio (SIC) plays a role similar to the signal-to-noise ratio (E/N0) for thermal noise and must be sufficiently high for reliable detection. While clutter statistics differ from thermal noise, SIC values might initially be approximated using E/N0 values when no other information is available. Notably, range dependence for clutter detection is linear, unlike the fourth power dependence for noise detection. Therefore, a narrow radar beam and short pulse width are crucial for detecting targets in clutter. If multiple hits are received per scan and the clutter is correlated from pulse to pulse, no improvement in SIC is achieved, unlike in thermal noise scenarios [4].

1.8 Range Ambiguity

Range ambiguity in radar occurs when the radar cannot accurately determine the target's actual distance due to the periodic nature of radar pulses. Radars operate by transmitting short pulses of electromagnetic waves, then pausing to wait for any returning echoes from targets. The time delay of the echo helps calculate the distance to the target.

When the radar continuously sends out pulses, an echo from a previous pulse may return after a subsequent pulse is transmitted. The radar could mistake this echo for one associated with the latest pulse, leading to an incorrect, shorter-range estimate for the target.

When the radar estimates the range R2, it assumes the echo came from the most recent pulse, even though the echo could have originated from an earlier transmission, corresponding to range R1. The true distance to the target could be any of the distances:

$$R_2 + k(R_2 - R_1) \tag{1.12}$$

where k is any positive integer. Because the radar cannot distinguish between these possible ranges based solely on the time of the received echo, it introduces uncertainty in determining the correct target distance.

To prevent range ambiguity, the pulse repetition interval (PRI) “the time between consecutive pulses” must be properly chosen. By increasing the PRI, the radar ensures that echoes from distant targets do not overlap with those from closer ones in the next pulse cycle. The maximum unambiguous range Rmax is expressed as:

$$R_{max} = \frac{c.PRI}{2} \tag{1.13}$$

where c represents the speed of light[4].

1.9 Fluctuating target models

When a radar signal encounters a target, the power reflected from the target depends on its radar cross section (or area). The RCS is related to the power Pr received by the target when it is immersed in a space with a power flux density W by the expression,

$$P_r = A_e W \tag{1.14}$$

Where Ae is the equivalent area of the target. Equation above shows that the larger the RCS, the higher the amplitude of the reflected signal.

In general, the RCS of a real target is not constant over time when the target is in motion. As a result, when the target enters the radar beam, it receives a group of pulses for the duration of the illumination, and consequently reflects a train of pulses whose amplitude fluctuates more or less slowly from one pulse to the next.

Depending on their speed, two types of RCS fluctuations can be distinguished. The fluctuations are called scan-to-scan if the amplitude of the reflected pulses located in the same group is constant, but can be variable from one group to another, i.e. from one scan to another; they are pulse-to-pulse if this amplitude varies from one pulse to another in the same group. In the first case, the RCS fluctuates with each scan and in the second case with each pulse.

To model target fluctuation, there are mainly four cases, called Swerling cases, corresponding to mathematical models describing the envelope of the echo

amplitude distribution. These models are numbered 1 to 4 with an additional model 5 (or 0) less used than the previous ones[1]

1.9.1 Swerling model 1

In the Swerling Model 1, the fluctuations are sweeping. The envelope of the pulse train is a random variable with a Rayleigh probability density:

$$P_s = \frac{1}{m_s} e^{-(s/m_s)} \quad , s \geq 0 \tag{1.15}$$

Where S is the signal-to-noise power ratio and m_s is the mean of S. In addition, the initial phases of the pulses are statistically independent random variables with uniform density probabilities.

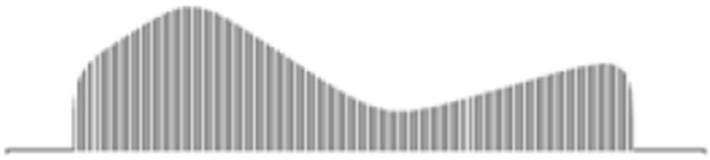

Figure 1.12 Swerling 1

1.9.2 Swerling model 2

In this case, the fluctuations are pulse to pulse. The amplitude of each pulse, instead of each group of pulses, is an independent random variable with the same density as case 1. The initial phases are also independent random variables with uniform densities.

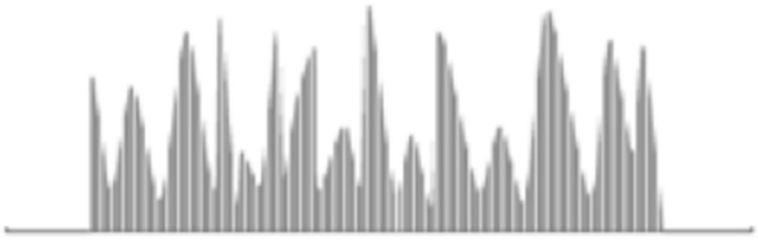

Figure 1.13 Swerling 2

1.9.3 Swerling model 3

In this case, the fluctuations are sweeping. Model 3 differs from model 1 in the density probability:

$$P_s = \frac{4s}{m_s\text{^}2} e^{-(2s/m_s)} \quad , s \geq 0 \tag{1.16}$$

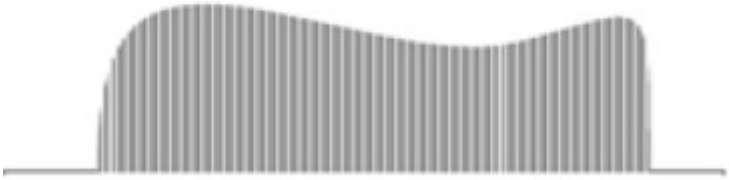

Figure 1.14 Swerling 3

1.9.4 Swerling model 4

In this case, the fluctuations are pulse to pulse. Model 4 is similar to model 2 but Equation 1.15 gives its density probability.

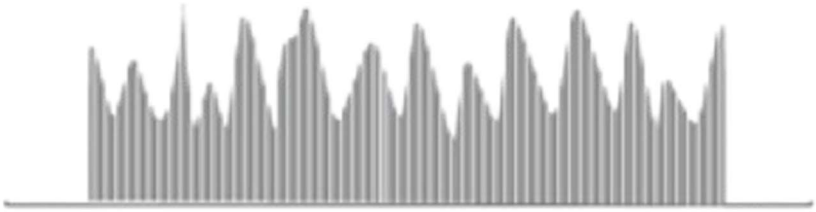

Figure 1.15 Swerling 4

1.9.5 Swerling model 5 (or 0)

Model 5, also called Model 0, corresponds to non-fluctuating targets. The amplitude of the received signal is assumed to be constant and unknown. This case is less used than the previous cases.

In practice, cases 1 and 2 correspond to targets consisting of many independent reflectors of comparable RCS (large aircraft) and cases 3 and 4 to targets having a dominant, non-fluctuating RCS reflector with other smaller, independent reflectors (missiles).

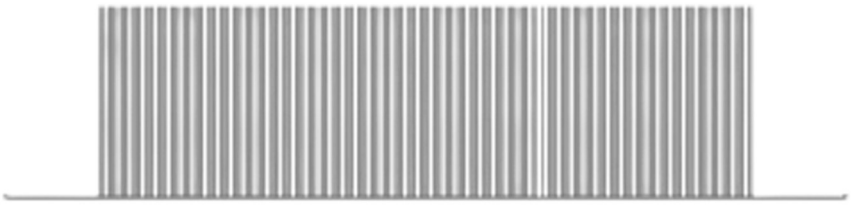

Figure 1.16 Swerling 5

1.10 Signal processing phase

The major blocks—the modulator, the transmitter, the receiver, the signal processor, the data processor, and the display—and their functions are now briefly described.

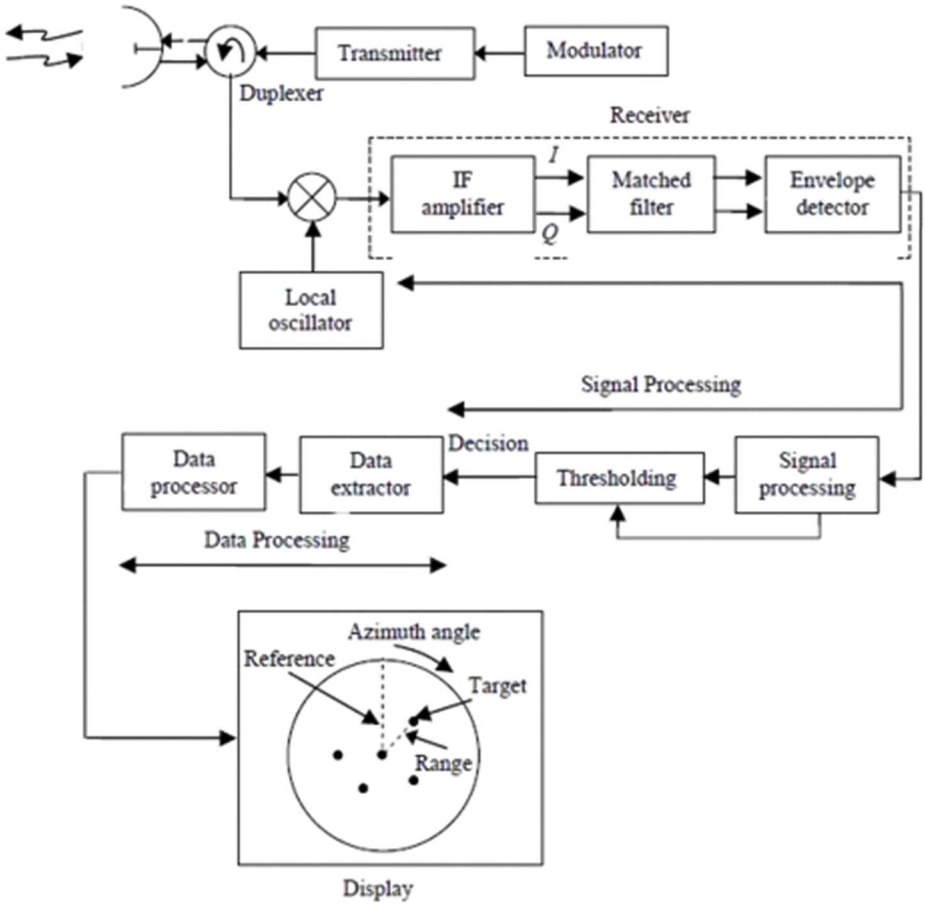

Figure 1.17 Signal and data processing in a modern pulse radar system.

The Modulator Upon reception of each timing pulse, the modulator produces a high-pulse direct current and supplies it to the transmitter.

The Transmitter The transmitter is a high-power oscillator. It generates a high peak power coherent train of pulses to illuminate the target.

The Receiver Typically, the receiver is of a superheterodyne type. It provides frequency conversion (to a lower frequency called intermediate frequency, IF), interference rejection, and low-noise amplification. Noise reduction is an important consideration in radar receiver design, and it is accomplished by a matched filter that maximizes the SNR at the output.

Signal Processor This device processes the target echoes and interfering signals to increase the signal-to-interference ratio. The operations may be pulse compression, Doppler range clutter suppression techniques, and CFAR processing. This is the part that will be developed in detail. However, we say briefly that the CFAR circuit keeps the rate of occurrence of false decisions (alarms) due to background noise and clutter at a constant and relatively low rate. This prevents saturation of the system and/or user. It estimates the noise and clutter level from a number of range, Doppler, and/or azimuth cells to allow the threshold to be set correctly.

Data Processor It provides the target measurements in range, angle (azimuth and elevation), radial velocity, and possibly the target signature.

Display The output is generally conveyed to a display to visualize the information contained in the target echo signal in a form suitable for operator action and interpretation. *The plan position indicator* (PPI) is the usual display employed in the radar receiver, and it indicates the range and azimuth of a detected target.

When the transmitter and the receiver are in separate locations ($Rb \neq 0$), this is called a *bistatic* radar. In this case, the ranges $R1$ and $R2$ may not be the same. A *multistatic* radar is a radar with one transmitting antenna, but many receiving stations, all in a network. Most radars nowadays are *active* and of *pulse* type; that is, the radars have a transmitter, and the signal transmitted is a pulse [2].

Conclusion

In this chapter we have presented the different basic parameters of a radar system, the main components of a radar are: transmitter, receiver, antenna, detector and display. The radar equation is used to calculate the range of a radar, knowing the technical characteristics of the radar. The Doppler effect is used to estimate the radial speed of a target and to distinguish between moving and stationary targets. A proper limitation of the range of a radar avoids ambiguity in the estimation of the distance to targets. Swerling models are models of fluctuating targets and are used in estimating the performance of radar detectors. The decision whether a target is present or not depends on the comparison of the test sample to a threshold.

In the following we will study the techniques of one part of radar signal processing, namely detection.

CHAPTER 02

Detection Fundamentals

Summary

This chapter will introduce the basic concepts of detection theory, firstly the detection decision criteria, and then we look at the detection techniques which represent the foundation for the further construction of this project.

2 Detection fundamentals

2.1 Radar Detection as Hypothesis Testing

For radar measurements, there are two possible hypotheses:

1. The measurement is solely due to interference (null hypothesis H0).

2. The measurement is due to both interference and target echoes (non-null hypothesis H1).

The detection process evaluates each radar measurement and decides which hypothesis best explains it. If H0 is more suitable, the system concludes that no target is present at the specified range, angle, or Doppler coordinates. Conversely, if H1 is more appropriate, the system determines that a target is present [1].

The decision between the two hypotheses relies on statistical decision theory, using probability density functions (PDFs) to describe the measurements. For a given sample y, two PDFs are needed:

py(y|H0): PDF of y if no target is present.

py(y|H1): PDF of y if a target is present.

A crucial aspect of the detection problem involves developing models for the two PDFs. Radar performance analysis hinges on accurately estimating these PDFs for the specific system and scenario. Much of radar system design focuses on adjusting these PDFs to achieve optimal detection performance. In practice, detection is based on N data samples yn, which form a column vector y.

$$y \equiv [y_0 \cdots y_{N-1}] \tag{2.1}$$

The N-dimensional joint PDFs py(y|H0) and py(y|H1) are then used. Assuming the two PDFs are successfully modeled, the following probabilities of interest can be defined:

Probability of Detection PD: The probability that a target is declared (i.e., H1 is chosen) when a target is in fact present.

Probability of False Alarm PFA: The probability that a target is declared (i.e., H1 is chosen) when a target is in fact not present

Probability of Miss PM: The probability that a target is not declared (i.e., H0 is chosen) when a target is in fact present.

Note that$P_M = 1 - P_D$. Therefore, knowing P_D and the probability of false alarm P_{FA} is sufficient to define all relevant probabilities. It is important to recognize that, due to the statistical nature of the problem, there is always a finite chance of making incorrect decisions [2].

2.2 The Neyman-Pearson Detection Rule

The next step in decision-making is to determine the optimal rule for choosing between the two hypotheses. This is a complex field. The Bayes optimization criterion assigns a cost or risk to each combination of the actual state (target present or not) and the decision (select H0 or H1). In radar, a common approach is the Neyman-Pearson criterion, a special case of the Bayes criterion. This criterion aims to maximize the probability of detection P_D while ensuring that the probability of false alarm P_{FA} does not exceed a specified limit. The achievable P_D and P_{FA} combinations depend on the radar system's quality and signal processing design. For a fixed system design, increasing P_D typically results in an increased P_{FA}. Radar designers decide the acceptable false alarm rate based on the consequences of acting on a false alarm, such as allocating radar resources to track a non-existent target or, in extreme cases, firing a weapon. Given that radars can make millions of detection decisions per second, P_{FA} values must be very low, typically between 10^{-4} and 10^{-8}, yet this can still result in false alarms every few seconds. Higher-level logic in downstream data processing is often used to mitigate the number and impact of false alarms.
In the context of decision-making based on measured data vectors y in an N-dimensional space, each vector represents a point. To establish a complete decision rule, every possible point in this space, corresponding to all combinations of N data values, must be assigned to either of two decisions: H0 (target absent) or H1 (target present). When the radar observes a specific set of data values y, it categorizes the observation as either indicating "target absent" or "target present" based on the preassigned decision for that particular y. The region where H1 is chosen is denoted as region 1, which may consist of disconnected parts [2].

The probabilities of detection (detecting the target when it is present) and false alarm (incorrectly declaring the target when it is absent) can be expressed generally as integrals of the joint probability density functions (PDFs) over region 1 in the N-dimensional space.

$$P_D = \int_{R_1} py(y \mid H1)\, dy \tag{2.2}$$

$$P_{FA} = \int_{R_1} py(y \mid H0)\, dy \tag{2.3}$$

Since probability density functions (PDFs) are always nonnegative, Equation (6.2) demonstrates that the probabilities of detection P_D and false alarm P_{FA} must either both increase or both decrease together. When region 1, the area corresponding to a decision of H1, expands to include more possible observations y, the integrals over this region cover more of the N-dimensional space, resulting

in higher values for both P_D and P_{FA}. Conversely, if region 1 contracts, both P_D and P_{FA} decrease.

To increase the detection probability, the false alarm probability must also increase. In other words, achieving a good balance involves assigning points to region 1 that add more to the probability mass of P_D than to P_{FA}. If the system can be designed such that the PDFs $py(y \mid H1)$ and $py(y \mid H0)$ are largely disjoint, distinguishing between the two decisions becomes easier and more effective [2]

2.3 The Likelihood Ratio Test

The Neyman-Pearson criterion aims to achieve the optimal detection performance while ensuring that the false alarm probability remains within an acceptable limit. Therefore, the Neyman-Pearson decision rule is designed to chose R_1 so that P_D is maximized, subject to

$$P_{FA} \leq \alpha \tag{2.4}$$

where α is the maximum allowable false alarm probability. This optimization problem is solved by the method of Lagrange multipliers. Construct the function

$$F \equiv P_D + \lambda(P_{FA} - \alpha) \tag{2.5}$$

To find the optimum solution, maximize F and then choose λ to satisfy the constraint criterion PFA = α. Substituting (2.2) and (2.3) into Eq. (2.5)

$$F = \int_{R_1} py(y \mid H1)\, dy + \lambda\left(\int_{R_1} py(y \mid H0)\, dy - \alpha\right)$$

$$F = -\lambda\alpha + \int_{R_1} \{py(y \mid H1) + \lambda py(y \mid H0)\}\, dy \tag{2.6}$$

The design variable in this context is the selection of region 1. In the second line of (2.6), the first term remains constant regardless of the choice of region 1. Thus, to maximize F, the integral over region 1 must be maximized. Given that λ can be negative, the integrand can be positive or negative depending on the values of λ and the relative values of py(y|H0) and py(y|H1). To maximize the integral, region 1 should include all points in the N-dimensional space $py(y \mid H1) + \lambda py(y \mid H0) > 0$. In other words, region 1 should consist of all points y where $py(y \mid H1) > -\lambda py(y \mid H0)$. This directly leads to the decision rule.

$$\frac{py(y|H1)}{py(y|H0)} \gtrless -\lambda \tag{2.7}$$

Equation (2.7), known as the likelihood ratio test (LRT), provides a decision-making rule under the Neyman-Pearson criterion for determining whether a target is present based on observed data y and a threshold $-\lambda$. The LRT states that the

ratio of the two probability density functions (PDFs) evaluated at y should be compared to this threshold. If the ratio exceeds the threshold, hypothesis H1 (target present) is chosen; otherwise, hypothesis H0 (target not present) is chosen. This test ensures that the probability of a false alarm does not exceed the specified design value P_{FA} . Implementing the LRT requires models of $py(\, y \mid H1\,)$and py $(\, y \mid H0\,)$, and it specifies the data processing operations needed on y. The LRT is fundamental in detection theory and statistical hypothesis testing, similar to the Fourier transform in signal processing, and is also the optimal solution under various decision criteria. The LRT can be conveniently expressed as follows:

$$\Lambda(y) \gtrless \eta \tag{2.8}$$

Equation (6.6) defines the likelihood $\Lambda(y)$. Applying a monotone increasing transformation, such as the natural logarithm, to both sides simplifies the computations, resulting in the log likelihood ratio test.

In detecting a constant in zero-mean Gaussian noise σ_w^2, Let w be a vector of independent identically distributed (i.i.d.) zero mean Gaussian random variables. Under hypothesis H0, the data vector y= w follows an N -dimensional normal distribution. Under hypothesis H1, y=m+w shifts the distribution to a nonzero positive mean, where m > 0.

H0: y∽N $(0_{N,}\sigma_w^2 I_N)$

H1: y∽N $(\mathrm{m}1_{N,}\sigma_w^2 I_N)$

where m > 0 and $0_{N,}$ $1_{N,}$ and I_N are, respectively, a vector of N zeros, a vector of N ones, and the identity matrix of order N. The model of the required PDFs is therefore:

$$py(\, y \mid H0\,)\, dy = \prod_{n=0}^{N-1} \frac{1}{\sqrt{2\pi\sigma_w^2}} e^{\left\{\frac{-1}{2}\left(\frac{y_n}{\sigma_w}\right)^2\right\}}$$

$$py(\, y \mid H1\,)\, dy = \prod_{n=0}^{N-1} \frac{1}{\sqrt{2\pi\sigma_w^2}} e^{\left\{\frac{-1}{2}\left(\frac{y_n - m}{\sigma_w}\right)^2\right\}} \tag{2.9}$$

The likelihood ratio Λ(y) and the log-likelihood ratio can be directly

computed from (2.9):

$$\Lambda(y) = \frac{\prod_{n=0}^{N-1} e^{\left\{\frac{-1}{2}\left(\frac{y_n}{\sigma_w}\right)^2\right\}}}{\prod_{n=0}^{N-1} e^{\left\{\frac{-1}{2}\left(\frac{y_n}{\sigma_w}\right)^2\right\}}} \tag{2.10}$$

$$\ln\Lambda(y) = \frac{1}{\sigma_w^2}\sum_{n=0}^{N-1} m y_n - \frac{1}{2\sigma_w^2}\sum_{n=0}^{N-1} m^2 \tag{2.11}$$

Because of its simpler form, the log-likelihood ratio will be used. Substituting (2.11) into (2.8) and rearranging gives the decision rule:

$$\sum_{n=0}^{N-1} y_n \gtrless \frac{\sigma_w^2}{m} \ln(-\lambda) + \frac{N_m}{2} \equiv T \tag{2.12}$$

The log-likelihood ratio simplifies the decision rule to comparing the sum of data samples $\sum y_n$ to a threshold T. This method avoids explicitly evaluating PDFs and specifying regions in N-space. The term $\sum y_n$, known as the sufficient statistic $\gamma(y)$, encapsulates all necessary information for the likelihood ratio, making it as effective as the original data for Neyman-Pearson optimal decisions.

$$\gamma(y) \gtrless T \tag{2.13}$$

The concept of a sufficient statistic is essential, encapsulating all useful information in a single coordinate. To determine the threshold $\eta = -\lambda$ that ensures $P_{FA} = \alpha$, one must express P_{FA} in terms of the likelihood ratio Λor the sufficient statistic ϒ and solve for η or T.

$$\begin{aligned} \alpha = P_{FA} &= \frac{1}{\sqrt{\pi}} \int_{T/\sqrt{2N\beta^2}}^{+\infty} e^{-t^2}\, dt \\ &= \frac{1}{2}\left[1 - \operatorname{erf}\left(\frac{T}{\sqrt{2N\beta^2}}\right)\right] \end{aligned} \tag{2.14}$$

Eq. (2.14) can be solved to obtain the threshold T in terms of the tabulated inverse error function:

$$T = \sqrt{2N\beta^2}\, \operatorname{erf}^{-1}(1 - 2P_{FA}) \tag{2.15}$$

Equations (2.14) and (2.15) explain the relationship between the false alarm probability P_{FA} and the threshold T. To perform the likelihood ratio test (LRT) using the sufficient statistic ϒ(y), we sum the data samples and compute T based on the number of samples, noise variance, and desired P_{FA}. The detector's performance is assessed by creating a receiver operating characteristic (ROC) curve, which relates the probability of detection P_D to P_{FA}, noise power, and the constant m. To find P_D, we determine the probability density function of ϒ under H0 and integrate from the threshold to infinity. Under H1, the mean of ϒchanges to Nm, and we can express the relationship between P_D and P_{FA} using the signal-to-noise ratio, leading to a simplified form of the error function for performance evaluation [2].

$$P_D = \frac{1}{2}[1 - \text{erf}\left\{erf^{-1}(1 - 2P_{fa}) - \sqrt{x/2}\right\}]$$

$$= \frac{1}{2}\text{erf}\,[erf^{-1}(2P_{fa}) - \sqrt{x/2}] \quad (2.16)$$

2.4 Bayes' criterion

Bayes' criterion assumes that the four possible events(D0,H0), (D0,H1), (D1,H0), (D1,H1) at the end of a decision, where (Di,Hi) ; i = 0,1 ; j = 0,1 means that the decision Di is taken when the hypothesis Hj is true, are each associated with a cost Cij which in practice represents the cost incurred by the corresponding decision. In addition, the priori probabilities of the realizations of the hypothesis H0 and H1 are assumed to be known.
This criterion then determines the decision rule by minimising the average cost, called risk and noted R [2].

$$R = C_{00}P(D_0, H_0) + C_{01}P(D_0, H_1) + C_{10}P(D_1, H_0) + C_{11}P(D_1, H_1) \quad (2.17)$$

According to Bayes' law, we have

Where
$$P(D_i, H_i) = P(D_i|H_i)P(H_j)$$
$$P(H_j) = P_j \,, j = 0, 1 \quad (2.18)$$

is the a priori probability of the hypothesis Hj. Substituting (2.17) into (2.18), we get

$$R = C_{00}P(D_0, H_0)P_0 + C_{01}P(D_0, H_1)P_1 + C_{10}P(D_1, H_0)P_0 + C_{11}P(D_1, H_1) \quad (2.19)$$

Finally, we replace the expressions for Pd and Pfa mentioned in hypothesis testing, we obtain

$$\mathbf{R = P_0C_{00} + P_1C_{01} + \int_{Z_1}^{Z_0} \left[P_0(C_{10} - C_{00})f_{(y|H_0)}(y|H_0) - P_1(C_{10} - C_{00})f_{(y|H_0)}(y|H_0)\right] dy}$$

In this expression, the term C00 P0+C01 P1 does not depend on the domains Z0 and Z1. The decision rule is obtained by assigning to the domain Z1 the set of values of y(t) such that the integrant is negative

$$P_0(C_{10} - C_{00})f_{(y|H_0)}(y|H_0) - P_1(C_{01} - C_{11})f_{(y|H_1)}(y|H_1) < 0 \quad (2.20)$$

Since C10-C00>0 and C10-C00>0, the cost of a wrong decision is higher than the cost of a right decision, the decision rule finally becomes

$$\frac{f_{(y|H_1)}(y|H_1) >}{f_{(y|H_0)}(y|H_1) <} \frac{P_0(C_{10}-C_{00})}{P_0(C_{01}-C_{11})} \tag{2.21}$$

The first member of the rule (2.21) is called the likelihood ratio and denoted Λ(y)

$$\Lambda(y) = \frac{f_{(y|H_1)}(y|H_1)}{f_{(y|H_0)}(y|H_0)} \tag{2.22}$$

and the second member is the detection threshold, denoted η, relative to Λ(y). Thus, the is simply written as

$$\Lambda(y) \underset{H_0}{\overset{H_1}{\gtrless}} \eta \tag{2.23}$$

2.5 Parameter Estimation

Parameter estimation is a statistical process used to infer the values of unknown parameters in a model based on observed data. Given a set of noisy or incomplete measurements, the goal is to determine the most likely values of these parameters that characterize the underlying system or distribution.

There are two main types of parameter estimation:

- Maximum Likelihood Estimation (MLE): Estimates non-random parameters by finding the parameter values that maximize the likelihood of the observed data.
- Bayesian Estimation: Estimates random parameters by incorporating prior knowledge about the parameter distribution, leading to a posterior distribution based on both the prior and the observed data [2].

2.5.1 Maximum Likelihood Estimation

Maximum Likelihood Estimation (MLE) is a method used to estimate nonrandom parameters from a set of observed data. The idea is to find the parameter value that makes the observed data most probable.

Let Y1,Y2,…,YK be K independent and identically distributed (i.i.d.) observations of a random variable Y, where the true distribution of Y depends on an unknown parameter θ.

Let $f_{Y/\Theta}(y/\theta)$ be the conditional probability density function of the random variable Y, given the parameter θ. The density function depends on θ, and our goal is to estimate θ.

The likelihood function L(θ) represents the joint probability of observing the given data y1,y2,…,yK, assuming that the parameter θ is the true value. It is given by the product of the individual likelihoods for each observation:

$$L(\theta) = f_{Y|\Theta}(y_1|\theta) \cdot f_{Y|\Theta}(y_2|\theta) \cdot \cdots \cdot f_{Y|\Theta}(y_K|\theta) = \prod_{k=1}^{K} f_{Y|\Theta}(y_k|\theta). \tag{2.24}$$

This is the likelihood function, which expresses how likely the observed data is for a given value of θ.

To estimate θ, we seek the value $\hat{\theta}$ that maximizes the likelihood function L(θ). The estimator $\hat{\theta}$ that maximizes L(θ) is called the Maximum Likelihood Estimator (MLE).

However, it's often easier to work with the logarithm of the likelihood function (called the log-likelihood) since taking logarithms turns the product into a sum:

$$\ln L(\theta) = \sum_{k=1}^{K} \ln f_{Y|\Theta}(y_k|\theta) \tag{2.25}$$

Maximizing ln L(θ) gives the same result as maximizing L(θ) because the logarithmic function is monotonically increasing. Therefore, the MLE is obtained by solving the following equation (also called the likelihood equation):

$$\frac{\partial}{\partial\theta} \ln L(\theta) = 0. \tag{2.26}$$

This gives the necessary condition for $\hat{\theta}$ to be the maximum likelihood estimator [2].

2.6 Detection techniques

Radar detection techniques can be broadly categorized into classical and adaptive methods. In classical detection, a fixed threshold is used, whereas in adaptive detection, the threshold is continuously adjusted based on the noise level. This section of Chapter 2 introduces both techniques, focusing on adaptive detection. We begin by discussing traditional detection methods, where the threshold is fixed, highlighting their operational principles and primary drawbacks, which pave the way for understanding adaptive detection—the focus of this study.

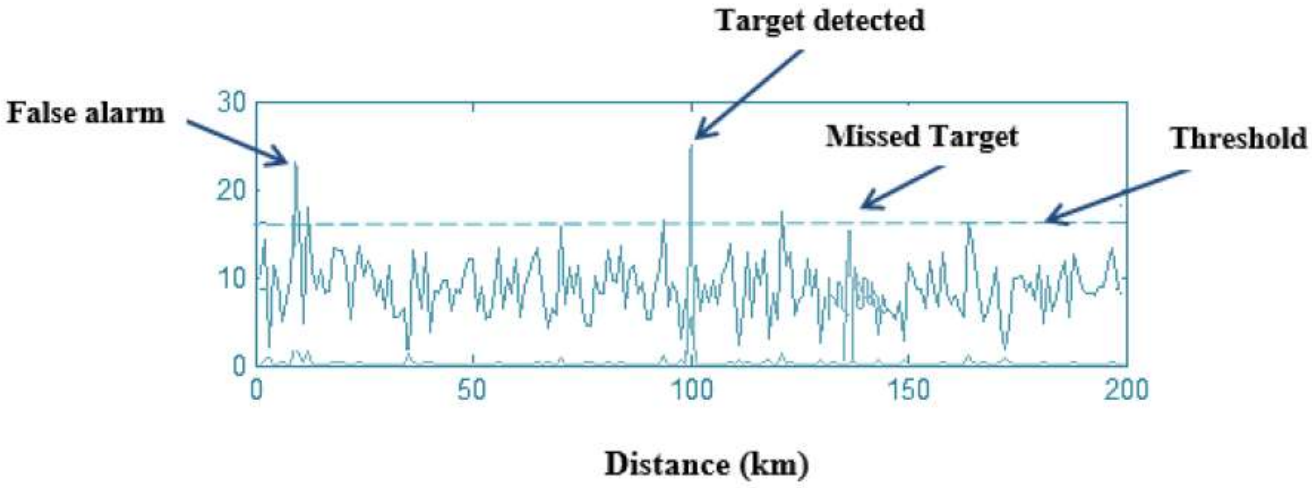

2.1 detection principle Figure

Before delving into the operation of conventional detectors, also known as fixed threshold detectors, it is important to understand how radar monitors its surveillance volume, which is the area of space under observation.

Radar emits pulses of duration τ, repeated at intervals of Tr, modulating a higher frequency carrier. If two targets in the same direction each produce their own echo, the radar cannot distinguish between them unless they are separated by a minimum distance, ΔR, known as range resolution, given by:

$$\Delta R = \frac{c\tau}{2} \tag{2.27}$$

where c is the speed of electromagnetic waves in the atmosphere. Additionally, the radar's beam, not being perfectly directional, has a certain angular width, which imposes angular resolution in both elevation and azimuth.

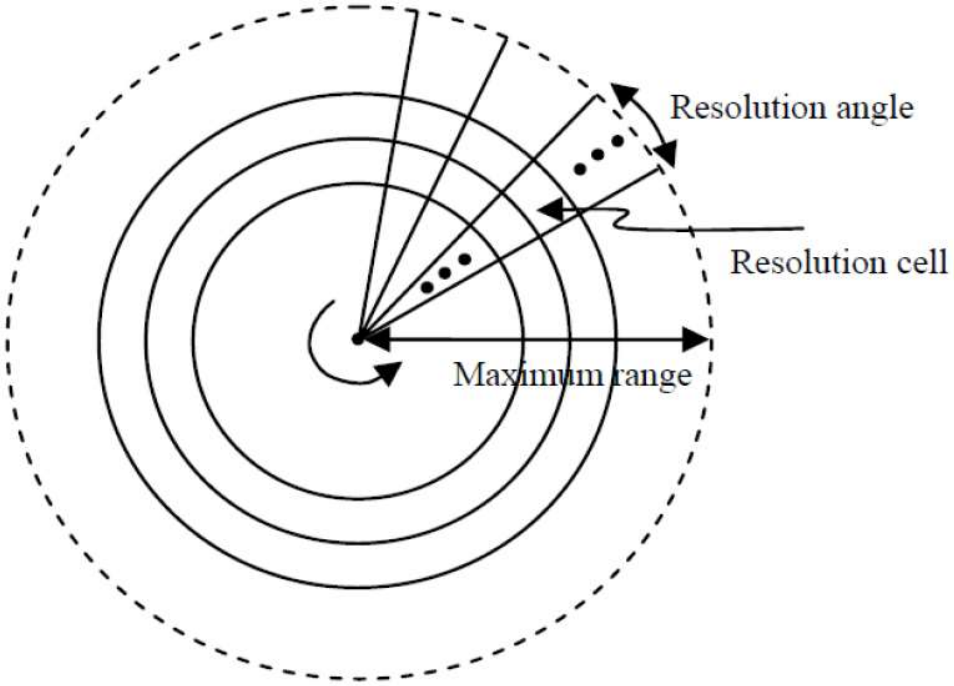

Figure 2.2 A Radar Scan

The radar's surveillance volume is divided into small adjacent regions known as cells. A target remains detectable at the same distance as long as it stays within the same cell, and two targets within the same cell cannot be distinguished.

When a target is within a cell of the surveillance volume, the radar illuminates this cell, causing the target to receive and reflect multiple successive pulses. These reflected pulses form a pulse train with variable amplitude. The detector receives several echoes from the same target, and the decision on target presence is made by comparing an estimated amplitude of these echoes to a detection threshold. The detector must therefore estimate the amplitude of the pulse train from the individual pulse amplitudes. This estimated amplitude is compared to the detection threshold to determine whether a target is present in the cell under test [2].

2.6.1 Optimal detection

The distribution of reflected pulse amplitudes depends on the model of target fluctuations. Numerous studies, particularly by Di Franco and Rubin, have shown that the optimal detector for white Gaussian noise is consistent across different Swerling cases. This optimal detector operates as follows: The received signal is passed through a single-pulse matched filter to maximize the signal-to-noise ratio. The signal from this filter is then fed into a quadratic detector, which extracts and squares the signal's envelope. The envelope is sampled at the pulse recurrence period, Tr. After the radar completes scanning the cell, N samples are obtained from the same target, each pulse contributing a sample. These N samples are summed, and the result, an estimate of the target's echo strength, is compared to a fixed threshold. If the sum exceeds the threshold, a target is detected in the cell (H1 is true); otherwise, the cell is deemed empty (H0 is true).

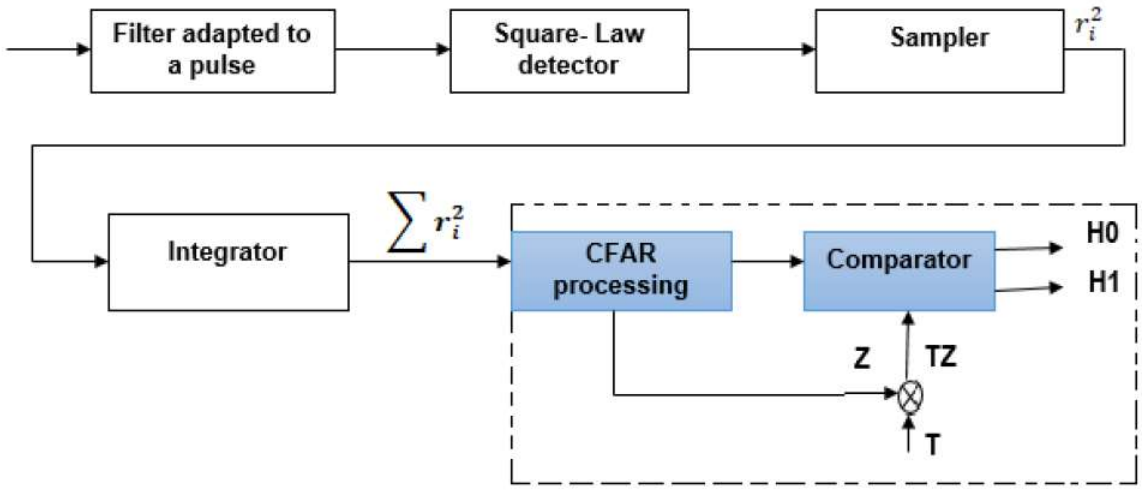

Figure 2.3 Diagram of a Conventional Detector

Radar detection involves a binary hypothesis test within an observation vector X of dimension N, where a known complex signal s, representing a target, is disrupted by additive clutter noise b. The binary hypotheses are:

$$H_0: X = b \qquad \text{(No Target present)}$$

$$H_1: X = s + b \qquad \text{(Target present)}$$

Here, Xi represents the secondary data, assumed to be independent and containing only clutter noise under hypothesis H0, which helps estimate the unknown clutter parameters. Under hypothesis H0, the received signal X contains only undesirable echoes, while under H1, it contains the target signal s embedded in clutter noise. The probability density functions under each hypothesis are given by $P_X(X/H_0)$ and $P_X(X/H_1)$, respectively [2].

Optimal detection aims to minimize two types of errors:

1. Miss (H0 is chosen when H1 is true), with probability:

$$P_M = P(H_0/H_1)=1-P_D \quad (2.28)$$

2. False alarm (H1 is chosen when H0 is true), with probability:

$$P_{fa} = P(H_1/H_0) \quad (2.29)$$

These probabilities are challenging to estimate unless the radar environment's statistics and the target's characteristics are well understood.

2.6.2 Fixed Threshold Detection

In radar systems, a decision must be made about the presence or absence of a target, with the output being a random process characterized by a probability density function (PDF). The presence of spurious noise introduces a risk of error in recognizing the useful signal, making it a statistical decision problem. Two hypotheses are considered:

H_0: The Target is absent (noise only)

H_1: The Target is present with noise

The detection problem can be summarized as follows:

Decision Hypothesis	**H0 (absence)**	**H1 (presence)**
$\boldsymbol{H_1}$	False alarm P_{fa}	Correct decision P_D
$\boldsymbol{H_0}$	Correct decision 1-P_{fa}	Incorrect decision 1-P_D

Table 2-1 Decision Hypothesis

The detection threshold is determined by setting the probability of false alarm. Once this probability is set, the threshold remains constant. If the noise power increases, the threshold does not adjust, leading to potential false alarms. The false alarm rate (number of false alarms per unit of time) can become intolerable. To address this issue, adaptive detection was developed.

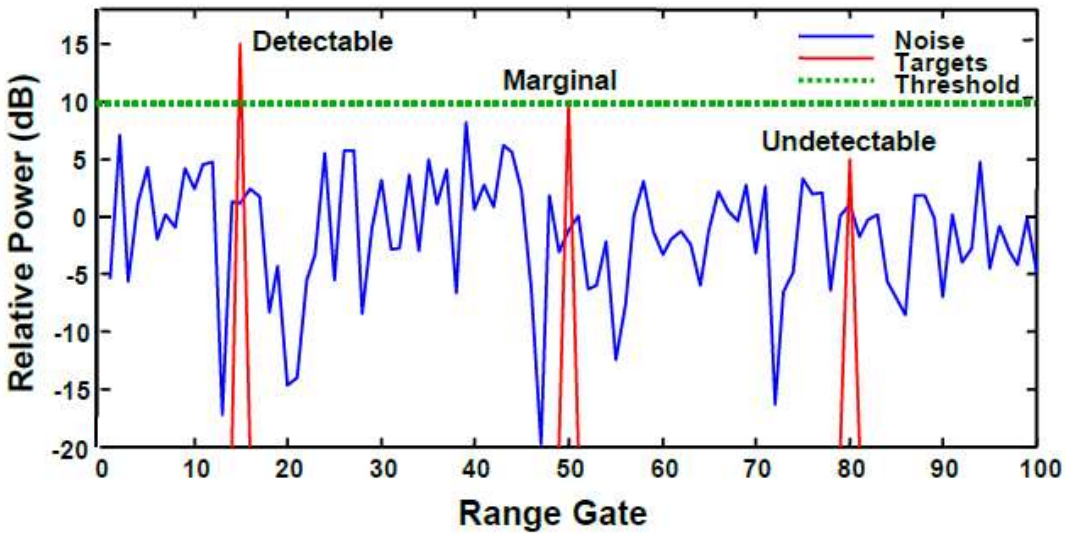

Figure 2.4 Principle of fixed threshold detection

Fixed threshold detection is becoming less common due to its susceptibility to high false alarm rates, which has led to the adoption of adaptive thresholding to maintain a Constant False Alarm Rate (CFAR). This adaptive threshold adjusts to fluctuations in the average clutter level [2].

2.6.3 Adaptive Threshold Detection

In radar systems, the goal is to detect the presence or absence of one or more targets, analyse the received signal, and obtain additional information such as the target's speed, altitude, and direction. The radar antenna emits pulses s(t) in the direction θ. If a target is present, the transmitted signal is reflected and received by the antenna with a delay time proportional to the distance d between the antenna and the target:

$$R(t) = \alpha\, s\big(t - \tau(d)\big) + b(t) \tag{2.30}$$

Where

$$\tau(d) = \frac{2d}{c} \tag{2.31}$$

α : depends on the target's altitude, reflection properties, distance, etc.

c: the speed of electromagnetic waves

b(t): white noise

This system addresses the decision problem between two hypotheses:

$H_0: R(t) = b(t)$ (No target)

$H_1: R(t) = \alpha\, s\big(t - \tau(d)\big) + b(t)$ (Target present)

Here, H0 corresponds to the absence of a target in the direction θ, and H1 corresponds to the presence of a target at a distance determined by τ(d).

Using fixed threshold detection can lead to a high number of false alarms due to the sensitivity of the false alarm probability to changes in clutter power. This challenge highlights the need for adaptive threshold detection [1].

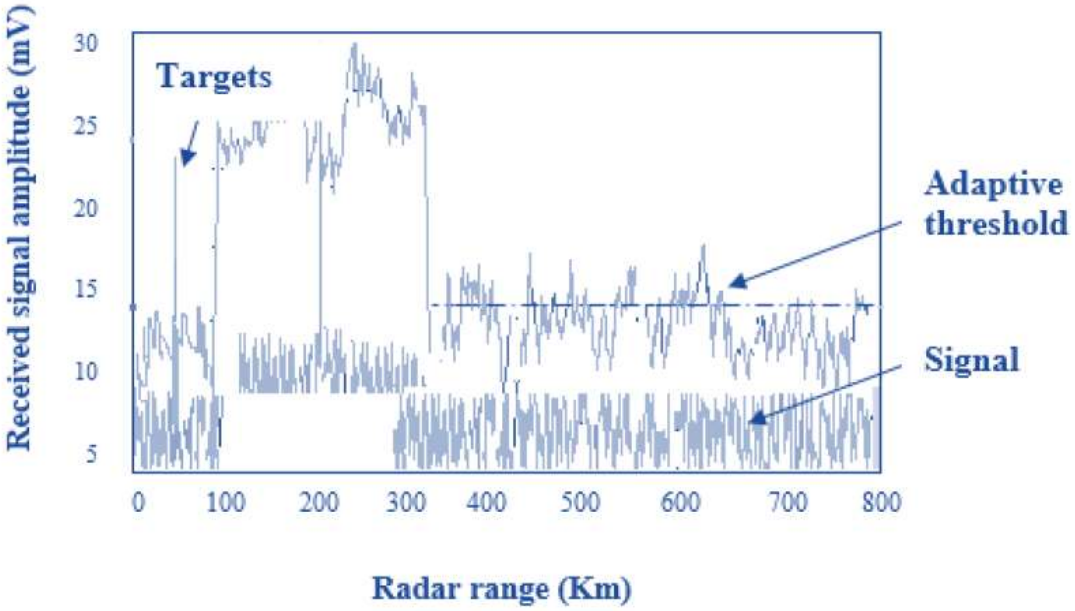

Figure 2.5 Principle of adaptive threshold detection

Conclusion

In this chapter, some basic notions of decision criteria detection have been presented, as well as the detection techniques used. As a result, we have seen that fixed threshold detection cannot be used in a non-homogeneous environment. To solve this problem, we resort to adaptive threshold detection, which ensures a Constant False Alarm Rate.

CHAPTER 03

Adaptive thresholding CFAR Detection

3 Adaptive thresholding CFAR Detection

3.1 Introduction

In signal detection, the primary objective is to design an optimal receiver structure based on a specific criterion relevant to the application. Ideally, these optimal detectors require a comprehensive statistical description of the input signals and noise. However, in practical scenarios, such information may not be available beforehand, and the statistics of the input data may change over time. These limitations necessitate the use of non-optimal detectors.

In real-world radar signal detection systems, the challenge is to automatically identify a target amidst thermal noise and clutter. Clutter refers to any unwanted radar signal from scatterers that are not of interest to the radar operator, such as reflections from terrain, sea, rain, birds, insects, and chaff. Chaff, consisting of metallic dipole reflectors, is released from aircraft to obscure the true target from radar. Although Doppler processing has reduced its effectiveness, it remains a concern for slow-moving targets. The operating environment of a radar, influenced by weather and physical location, makes the returned signals statistically nonstationary with an unknown variance at the receiver input.

The ideal detector, which employs a fixed threshold, is highly sensitive to the total noise variance (thermal noise plus clutter). Even a slight increase in total noise power can significantly raise the probability of false alarms by several orders of magnitude. For single pulse detection, the probability of false alarm can be expressed mathematically. This sensitivity underscores the need for adaptive detection strategies in practical radar systems [2].

$$P_F = \exp\left(\frac{-\gamma^2}{2\sigma^2}\right) \tag{3.1}$$

where γ is the threshold level and σ2 is the total noise variance. Let P_{Fd} be the design probability of false alarm based on a known variance σ_d^2. For a fixed threshold γ, the probability of false alarm in terms of the noise level and design probability of false alarm is obtained from (3.1) as

$$P_F = (P_{\mathrm{Fd}})^{\sigma_d^2/\sigma^2} \tag{3.2}$$

In radar systems, maintaining a constant false alarm rate (CFAR) is critical, especially when dealing with variable noise environments. The design value, denoted as Pfa, represents the target probability of false alarm. As shown in Figure (3.1), even a 3 dB increase in noise power can cause the actual probability of false alarm to surge by more than 1,000 times, which is unacceptable for both computer

and human data processing. This significant sensitivity to noise necessitates the use of adaptive threshold techniques to ensure CFAR while maximizing the probability of target detection.

To understand the practical aspects of adaptive threshold detection, it is essential to first grasp the basic principles of radar. Although radar concepts can be complex and are extensively covered in various books, this summary focuses on the fundamental aspects needed to comprehend adaptive thresholding CFAR detection. Following this, various adaptive CFAR techniques are discussed. The concept of adaptive CFAR detection is also explored in the context of mobile communications, particularly within code division multiple access (CDMA) systems. A brief overview of spread spectrum communication systems is provided to understand the applications and potential future developments of adaptive CFAR detection in these systems [2].

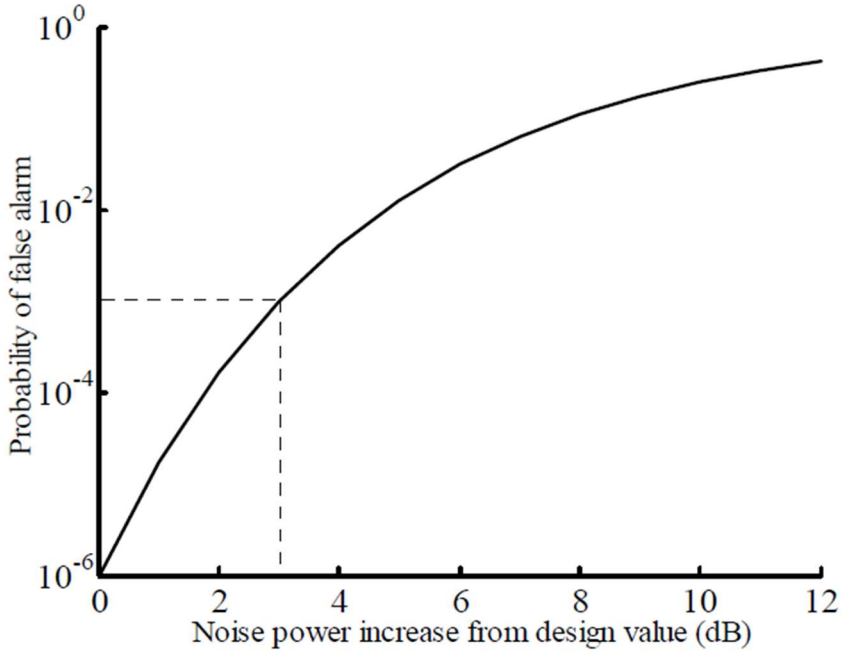

Figure 3.1 Effect of the noise power increase on the probability of false alarm for a fixed threshold; design Pfa =10−6.

3.2 Environment (background)

the environment is the medium which surrounds a system, in our case the environment is the medium crossed by the electromagnetic waves intervening of a radar and are reflected, about the reflected signals the environments of the radar differ, the behaviour of the signal emitted in a space differs according to the crossed medium for example: if a radar emits signals in a space the signals reflected from the sea or of a region that it rains or a forest it is not the same [1].

3.2.1 Homogenous background

this is the ideal environment for radar detection, it is the case of absence of clutter and interfering targets, the homogeneity is that the reflected signal samples are described by identically distributed independent exponential random variables

3.2.2 non homogenous background

When the reference window scans the environment in a given direction, different non-homogeneous situations can affect the configuration of the reference cells. These situations are caused by the presence of interfering targets (secondary targets) and/or clutter edges at the reference channel Figure (3.2).

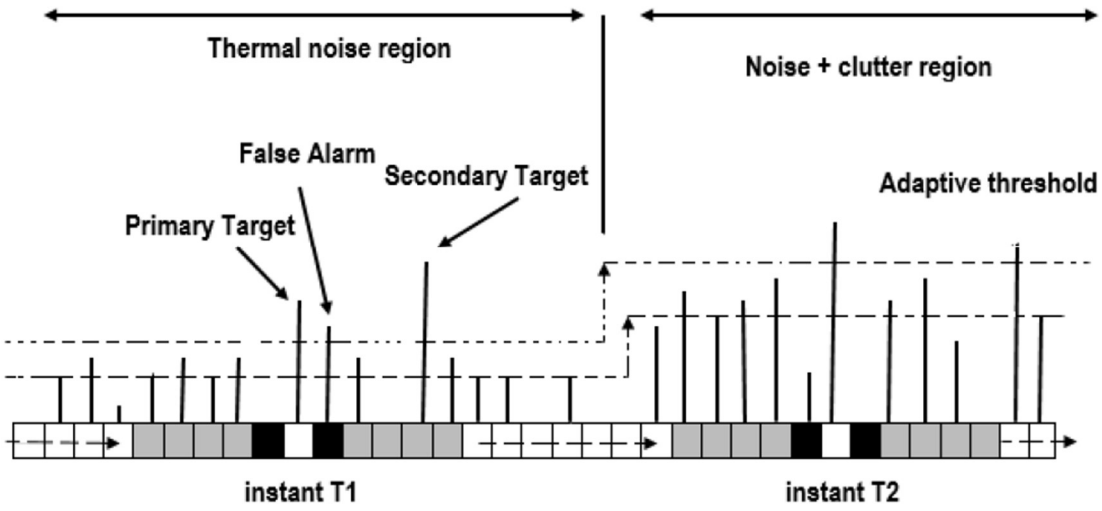

Figure 3.2 reference window scans a homogenous and non-homogenous environment

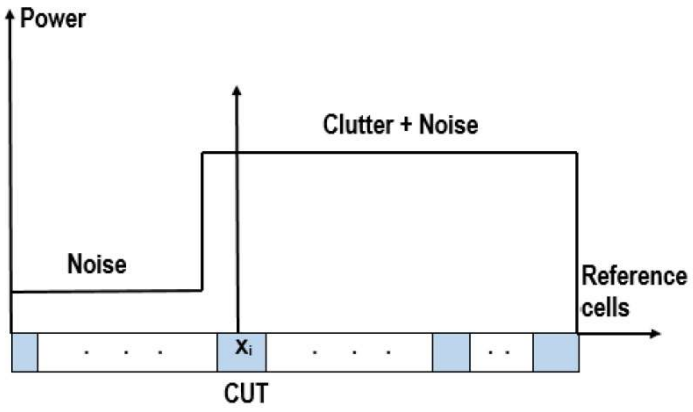

a. Cell under test is immersed in the clutter

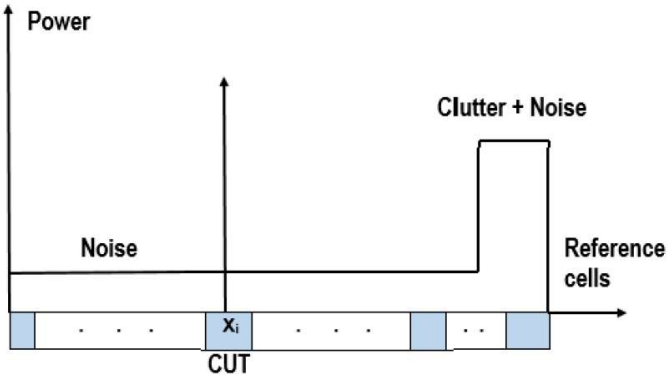

b. the cell under test is in thermal noise

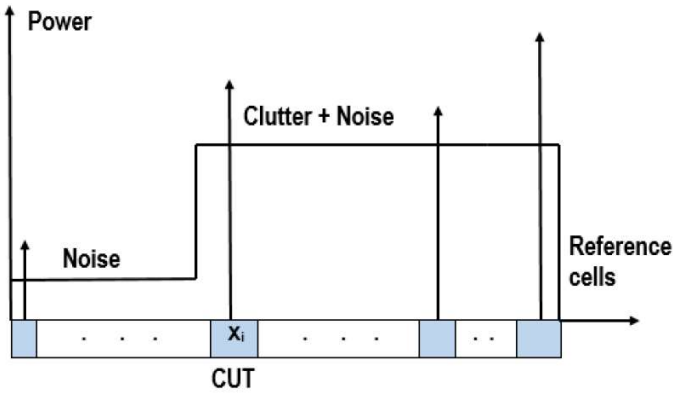

c. presence of clutter edge and interfering targets

Figure 3.3 different situations of non-homogenous environnement

3.3 Adaptive CFAR Detection

3.3.1 principles

When a target is present, the input signal at the radar receiver is a weakened version of the transmitted pulse, phase-shifted randomly and embedded in noise. A typical radar processor for a single-range cell aggregates the K samples from the matched filter output and compares this sum to a fixed threshold, as illustrated in Figure 3.4. In the case where the transmitted pulse is immersed in white Gaussian noise, the envelope of the clutter return signal follows a Rayleigh distribution. The optimal Neyman-Pearson detector for this scenario is depicted in Figure 3.5, with y(t) representing the received signal and ωc the carrier angular frequency. As seen in Figure 3.1, a slight increase in noise power can lead to an unacceptable rise in the probability of false alarms. Therefore, to manage the false alarm probability when the noise variance is unknown, [2]suggests using a reference channel. This channel provides an estimate of the noise environment, allowing the decision threshold to be adjusted accordingly [2].

The radar uses the range cells surrounding the cell under test as reference cells, as shown in Figure 3.6.

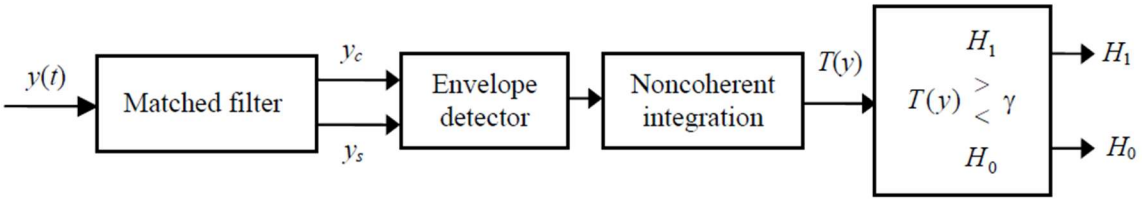

Figure 3.4 A scheme for a fixed threshold radar detection.

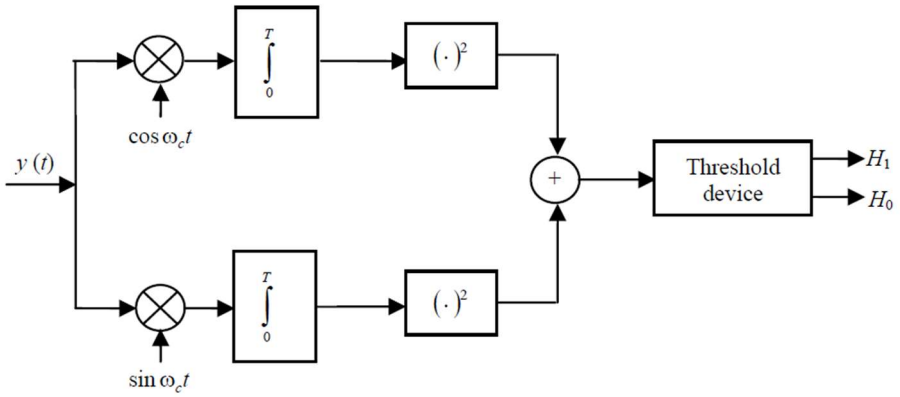

Figure 3.5 Optimum receiver, square realization.

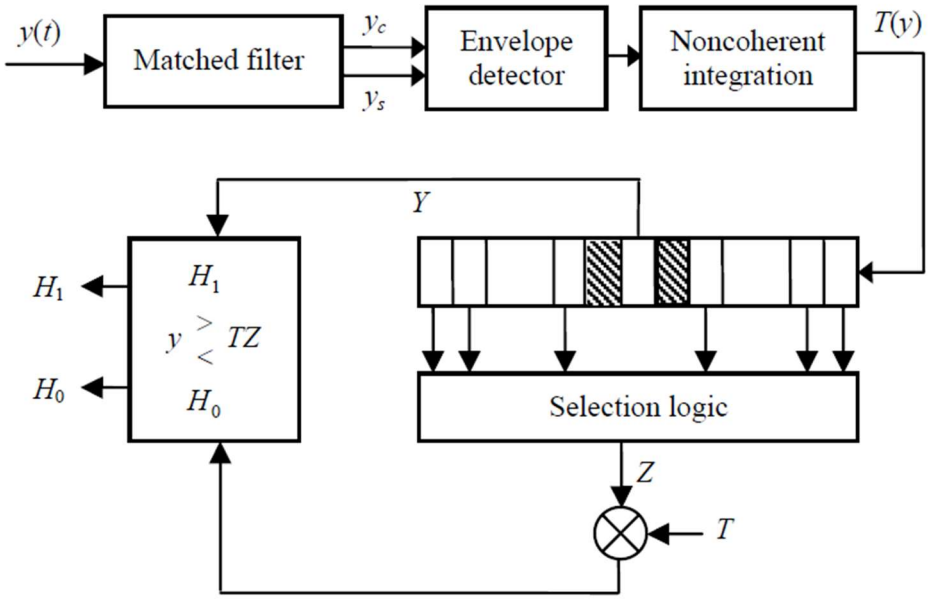

Figure 3.6 A scheme for an adaptive threshold radar detection.

3.3.2 Cell Averaging CFAR Detection

The Cell-Averaging Constant False Alarm Rate (CA-CFAR) detector is a widely used adaptive detection technique in radar systems. As proposed in [8], the CA-CFAR detector dynamically adjusts the detection threshold based on the noise environment, ensuring a constant false alarm rate regardless of varying background conditions.

In CA-CFAR, the adaptive threshold is derived from the arithmetic mean of the reference cells surrounding the Cell Under Test (CUT). The reference cells are used to estimate the noise level, and the arithmetic mean of these reference cell outputs serves as the detection threshold.

For a homogeneous background noise and independent and identically distributed (I.I.D) reference cell outputs, the arithmetic mean acts as the maximum likelihood estimate of the noise level. This adaptive approach ensures that the detection threshold can adapt to changes in the environment, maintaining a constant false alarm rate.

The noise observations for the CA-CFAR detector are obtained by sampling in both range and Doppler domains. As shown in Figure 3.7, the bandwidth of each Doppler filter (bandpass filter) is equal to the bandwidth of the transmitted rectangular pulse, denoted by B. The reference cells' outputs are sampled, and their arithmetic mean is used to compute the adaptive threshold. When the signal at the CUT exceeds this threshold, a target is detected [2].

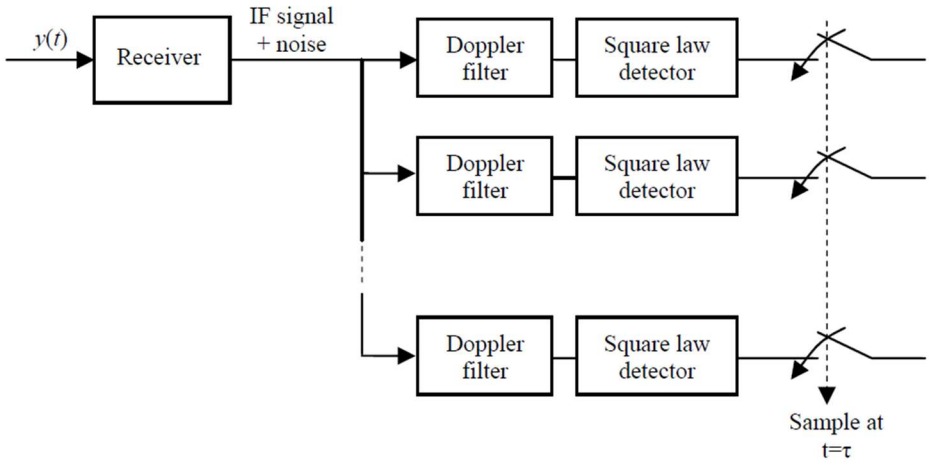

Figure 3.7 Range and Doppler sampling process.

Where $B = \frac{1}{\tau}$ and τ is the transmitted pulse width, each output from the square-law detector is sampled at intervals of τ seconds. This corresponds to a range

interval of $\frac{c\tau}{2}$. Consequently, each sample represents the output of a range-Doppler resolution cell with dimensions τ in time and $\frac{1}{\tau}$ in frequency. This results in a matrix of range and Doppler resolution cells, as illustrated in Figure 3.8.

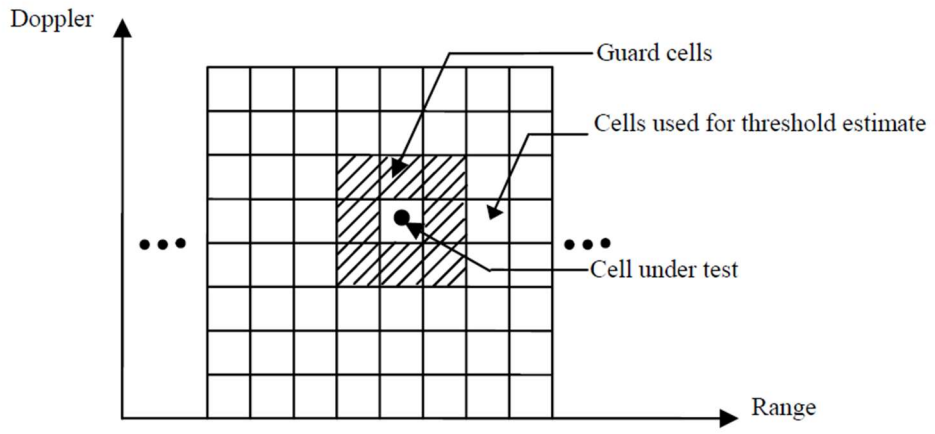

Figure 3.8 Matrix of range and Doppler cells.

For simplicity and without loss of generality, the CA-CFAR detector is depicted in Figure 3.9 for range cells only, focusing on a specific Doppler frequency.

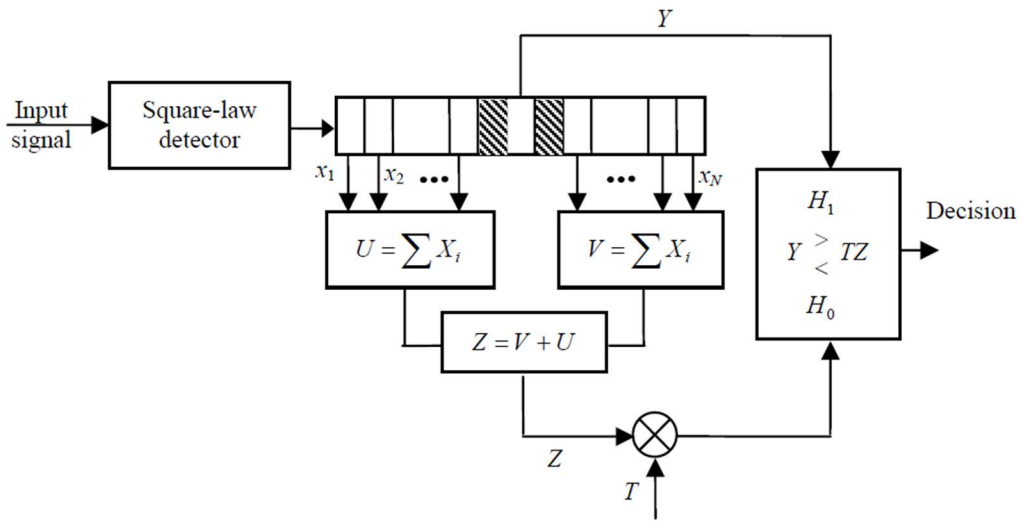

Figure 3.9 Cell averaging CFAR detector.

The system operates as follows: the output from the square-law detector is fed into a tapped delay line, forming the reference cells. This design prevents any spillover of signal energy from the test cell into adjacent range cells.

In a CA-CFAR detector, to avoid any signal energy spill from the test cell into adjacent range cells, which might affect the clutter power estimate, the adjacent cells, known as guard cells, are completely ignored. Each resolution cell is tested

independently to make a decision for the entire radar range. The cell under test is typically the central one.

The statistics of the reference windows U and V are derived from the sum of the leading and lagging cells, respectively, with each set containing N/2 cells. Therefore, a total of N noise samples are utilized to estimate the background environment. These reference windows U and V are combined to produce the clutter power estimate Z.

To keep the probability of false alarm Pf at a desired level, the adaptive threshold is scaled by a threshold multiplier T. The product TZ forms the adaptive threshold. The output Y from the test cell (the center tap) is then compared against this threshold to make a detection decision.

The primary target model at the test cell is assumed to be a slowly fluctuating target, modeled as a Swerling Case 1 target. The signal-to-noise ratio (SNR) of the target is denoted as S. It is further assumed that the total background noise is white Gaussian. Given that both noise and Rayleigh targets have Gaussian quadrature components, the output of the square-law detector follows an exponential probability density function (PDF). If the noise variance is σ2 , then the conditional density function of the output of the test cell is given by

$$f_{Y/H_i}(y/H_i) = \begin{cases} \frac{1}{2\sigma^2(1+S)} \exp[\frac{-y}{2\sigma^2(1+S)}], \text{for} H_1 \\ \frac{1}{2\sigma^2} \exp[\frac{-y}{2\sigma^2}], \text{for} H_0 \end{cases} \quad (3.3)$$

The hypothesis H0 represents the case of noise alone, while hypothesis H1 represents the noise plus target signal case. The probability of detection is given by

$$P_D = \int_0^\infty P(Y > \text{TZ}/Z, H_1) f_{Y/H_1}(y/H_1)\, dy = E_Z[P(Y > \text{TZ}/Z, H_1)] \quad (3.4)$$

where Z is the estimated homogeneous background noise power level, f Z (z) is the density function of Z, and EZ [·] is the expected value over all values of z. Substituting (3.3) into (3.4) and solving the integral, we obtain

$$P_D = E_Z\{\int_{T_Z}^\infty \frac{1}{2\sigma^2(1+S)} \exp[\frac{-y}{2\sigma^2(1+S)}]\, dy\} = E_Z\{\exp[\frac{-\text{TZ}}{2\sigma^2(1+S)}]\} = M_Z[\frac{T}{2\sigma^2(1+S)}] \quad (3.5)$$

where MZ (·) denotes the MGF of the random variable Z. We can obtain the probability of false alarm in a similar way, or by setting the target SNR, S, to zero to obtain:

$$P_F = M_Z(\frac{T}{2\sigma^2}) \tag{3.6}$$

Hence, for a design probability PF , the threshold multiplier T can be computed from (3.6). For the CA-CFAR detector, the reference window is:

$$Z = \sum_{i=1}^{N} X_i \tag{3.7}$$

with X i , i = 1, 2,K, N, independent and identically distributed random variables. From Chapter 2, the gamma density function G(α,β) given in (2.98) is:

$$f_x(x) = \frac{1}{\Gamma(\alpha)\beta^\alpha} x^{\alpha-1} e^{\frac{-x}{\beta}} \tag{3.8}$$

with MGF

$$M_x(t) = \frac{1}{(1-\beta t)^\alpha} \tag{3.9}$$

If we set α =1, we obtain the exponential distribution G(1,β) with density function

$$f_x(x) \frac{1}{\beta} e^{\frac{-x}{\beta}} \tag{3.10}$$

which is equivalent to $f_{Y/H_i}(y/H_i)$ given in (3.3), with β = 2σ² under hypothesis H0, and β = 2σ² (1+ S) under hypothesis H1 . Thus, using (3.9), the probability of false alarm of the distribution G (N, 2σ²) is

$$P_F = M_Z(\frac{T}{2\sigma^2}) = [1 - 2\sigma^2(\frac{T}{2\sigma^2})]^{-N} = \frac{1}{(1+T)^N} \tag{3.11}$$

The threshold multiplier is then:

$$T = -1 + P_F^{\frac{-1}{N}} \tag{3.12}$$

Replacing T / 2σ² by T /[2σ² (1+ S)] , the probability of detection is:

$$P_D = (1 + \frac{T}{1+S})^{-N} = (\frac{1+S}{1+S+T})^N \tag{3.13}$$

With the above cell averaging CFAR detector, assuming the data passed into the detector is from a single pulse, i.e., no pulse integration involved, the threshold factor can be written as

$$\alpha = N(P_{\text{fa}}^{\frac{-1}{N}} - 1) \tag{3.14}$$

where *Pfa* is the desired false alarm rate [3].

3.3.3 Order Statistic CFAR

An alternative to the cell-averaging CFAR is the rank-based or order statistic CFAR (OS CFAR). This approach, primarily designed to combat masking effects, retains the sliding window structure of CA CFAR, including optional guard cells. However, it forgoes averaging the reference window data to estimate interference levels. Instead, OS CFAR arranges the reference window data samples {x1,x2,...,xn}in ascending order to form a sequence {x(1),x(2),...,x(N)} The kth element in this ordered list is known as the kth order statistic. For instance, the first order statistic is the minimum value, the Nth is the maximum, and the (N/2)th is the median. In OS CFAR, a specific order statistic is chosen to represent the interference level, and the threshold is set as a multiple of this value [1].

This ranking from the minimum magnitude to the maximum magnitude ordered sequence is denoted as:

$$x(1) \leq x(2) \leq \ldots \leq x(k) \leq \ldots x(N). \tag{3.15}$$

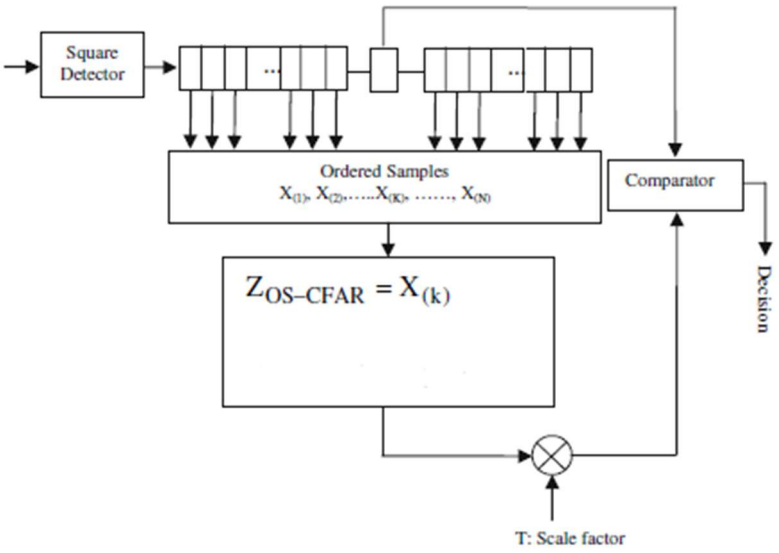

Figure 3.10 OS-CFAR Detector

From this sequence, the Kth ordered value, X(k), is selected to estimate the total noise power and scaled by a factor (T) to yield an adaptive threshold to which the output of the cell under test (CUT) is compared. Assuming that the target in the test cell is slowly fluctuating according to the Swerling I model and the background noise is Gaussian, the Pfai and Pdi are given by

$$\mathrm{Pd}_i = \int_0^{\infty} \Pr(Y > \mathrm{TZ}/Z\,, H_1) f_Z(Z)\, dZ \tag{3.16}$$

$$\text{Pfa}_i = \int_0^{\infty} \Pr(Y > \text{TZ}/Z, H_0) f_Z(Z)\, dZ \tag{3.17}$$

where Pr(Y > T Z/Z, Hi) is the conditional probability that Y > T Z given Z and Hi , i = 0, 1 and fz(Z) is the pdf of Z (the estimate of total noise power). Pdi and Pfai are given by:

$$\text{Pd}_i = \prod_{j=0}^{K-1} \frac{(N-j)}{N-j+\frac{T}{(1+S)}} \tag{3.18}$$

$$\text{Pfa}_i = \prod_{j=0}^{K-1} \frac{(N-j)}{(N-j+T)} \tag{3.19}$$

3.3.4 CMLD-K CFAR

The CMLD detector has the same first processing steps as the preceding one, except that the largest samples are censored, and the remaining K samples are combined to form the statistic Z as an estimate of the noise level in the CUT [6].

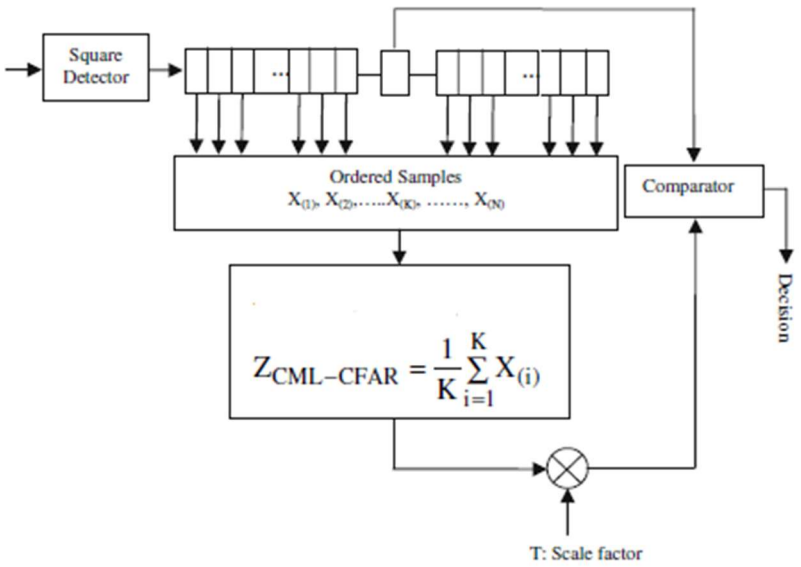

Figure 3.11 CML-CFAR Detector

Pdi and Pfai are, respectively, given by

$$\text{Pd}_i = \binom{N}{K} \prod_{j=1}^{K} \left[\frac{T}{1+S} + \frac{N-j+1}{K-j+1}\right]^{-1} \tag{3.20}$$

$$\text{Pfa}_i = \binom{N}{K} \prod_{j=1}^{K} \left[T + \frac{N-j+1}{K-j+1}\right]^{-1} \tag{3.21}$$

Conclusion

In this chapter, we have studied different types of CFAR detectors starting with the basic one which is the cell averaging after that the order statistic and the CMLD-k. Which will be used later on as the ground layer for customizing sensory systems.

CHAPTER 04

Optimization using Evolutionary Strategies

4 Optimization using Evolutionary Algorithms

4.1 introduction (Evolutionary Algorithms)

Many great inventions have been the result of bionics, i.e., the application of biological or natural principles to the study and design of human systems. We mimic bats to invent radar, fish to invent submarine, etc. The natural evolution of species could be looked at as a process of learning how to adapt to the environment and optimizing the fitness of the species. So, we could mimic the viewpoint of modern genetics, i.e., "survival of the fittest" principle, in designing, optimizing or learning algorithms. Enter EAs.

EAs are algorithms that perform optimization or learning tasks with the ability to evolve. They have three main characteristics:

• Population-based. EAs maintain a group of solutions, called a population, to optimize or learn the problem in a parallel way. The population is a basic principle of the evolutionary process.

• Fitness-oriented. Every solution in a population is called an individual. Every individual has its gene representation, called its code, and performance evaluation, called its fitness value. EAs prefer fitter individuals, which is the foundation of the optimization and convergence of the algorithms.

• Variation-driven. Individuals will undergo a number of variation operations to mimic genetic gene changes, which is fundamental to searching the solution space [11].

Since the 1960s, many algorithms with population-based, fitness-oriented, and variation-driven properties have been proposed. The timeline of the various EAS that will be introduced in this textbook is illustrated in Fig. 1.4.

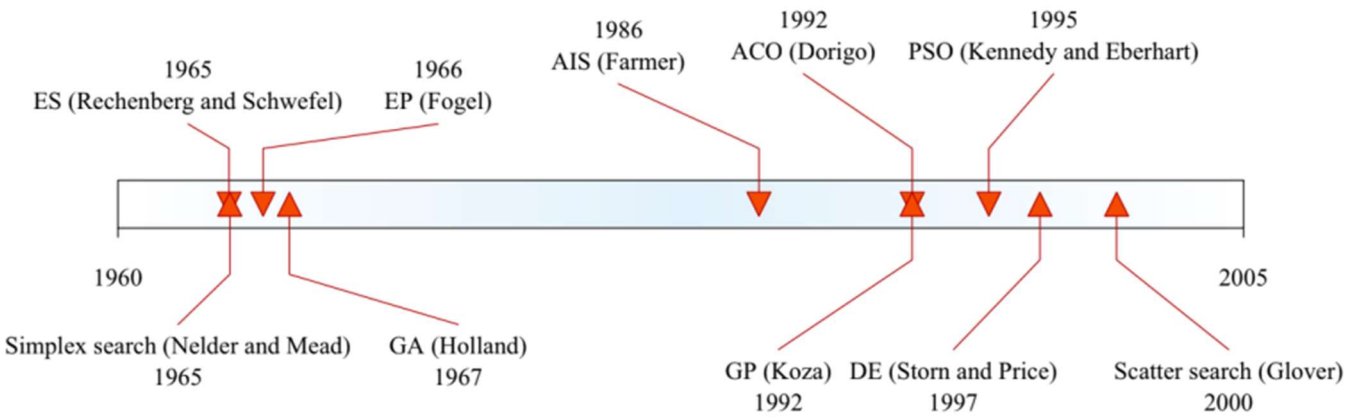

Figure 4.1 Timeline of various EAs

Evolutionary Algorithms (EAs) are a class of general stochastic search algorithms inspired by natural evolution, used across a wide range of applications such as optimization, adaptation, and learning. The significance of EAs in solving optimization problems is continually growing. However, implementing an EA involves various decisions, including the type of algorithm to use, the choice of operators, and the parameter settings for optimization. Yao [9] summarized a typical EA as follows:

1. Randomly generate the initial population P(0) and set i = 0;

2. Repeat until the population converges or the time limit is reached:

   a. Evaluate the fitness of each individual in P(i);

   b. Select parents from P(i) based on their fitness;

   c. Apply search operators to the parents to produce offspring, forming the next generation P(i + 1) from the offspring and possibly the parents.

Among the prevalent EA implementations for optimization problems are Genetic Algorithms (GAs) and Evolutionary Strategies (ESs). The primary differences between these methods lie in the representation of individuals, the operators used (mutation and crossover), and the selection/reproduction mechanisms, as discussed in [9,10].

4.2 Genetic Algorithm

4.2.1 Introduction

Genetic Algorithms (GAs) are computational models inspired by natural evolution, encoding potential solutions using a chromosome-like data structure. They employ recombination operators to preserve crucial information and are often used as function optimizers, though they apply to a wide range of problems. The process begins with a random population of chromosomes, evaluates their effectiveness, and allocates reproductive opportunities based on performance, favouring better solutions.

The concept of GAs was introduced by John Holland in his 1975 book, "Adaptation in Natural and Artificial Systems," which laid the foundation for the field of evolutionary computing. In the 1960s, similar ideas were developed by scientists like Ingo Rechenberg, Hans-Paul Schwefel, Bremermann, and Fogel, who emphasized mutation and selection, key concepts in neo-Darwinian evolution. However, it wasn't until the 1980s that evolutionary computing gained significant traction, partly due to the increasing availability of computational power.

Ken De Jong, a student of Holland, completed a doctoral thesis in 1975 that explored the optimization capabilities of GAs, sparking further studies and conferences. David Goldberg, another of Holland's students, produced an influential book in 1989, "Genetic Algorithms in Search, Optimization, and Machine Learning," which catalysed the rapid development of GA theory and applications.

While optimization was not the primary focus of Holland's work on adaptive systems, most GA research emphasizes this aspect. De Jong argued that GAs are not inherently function optimizers, suggesting that their primary value lies in adaptation. Despite this, GAs are widely used for optimization and are often successful in real-world applications.

Holland’s GA introduced recombination, setting it apart from earlier evolutionary algorithms that focused on mutation and resembled hill-climbing methods. This innovation parallels the development of heuristics in operational research during

the 1960s, where techniques like neighborhood search were used to explore combinatorial optimization problems by examining 'neighbors' of existing solutions [12].

4.2.2 Background

Genetic Algorithms (GAs) are inspired by natural evolutionary processes, specifically the concept of survival of the fittest. GAs initiate with a set of potential solutions and evolve these through successive generations to enhance their effectiveness. This evolutionary computation method mirrors how living organisms adapt and become more successful over time. It starts with an initial population of solutions and applies genetic operations like crossover and mutation to generate new offspring that inherit traits from parent solutions, with the aim of improving overall performance.

Chromosomes, composed of DNA, encode hereditary information through combinations of four bases: Adenine (A), Cytosine (C), Thymine (T), and Guanine (G). During reproduction, chromosomes undergo crossover, mixing genetic material from both parents, and occasionally mutation, where random errors introduce variations. While most mutations are harmful, some can result in beneficial traits, leading to the evolution of better-adapted species. Similarly, in GAs, these genetic variations are essential for exploring new solutions and achieving optimization in problem-solving [13].

4.2.3 Natural selection

In nature, the individual that has better survival traits will survive for a longer period of time. This in turn provides it a better chance to produce offspring with its genetic material. Therefore, after a long period of time, the entire population will consist of lots of genes from the superior individuals and less from the inferior individuals. In a sense, the fittest survived and the unfit died out. This force of nature is called natural selection.

The existence of competition among individuals of a species was recognized certainly before Darwin. The mistake made by the older theorists (like Lamarck) was that the environment had an effect on an individual. That is, the environment will force an individual to adapt to it. The molecular explanation of evolution proves that this is biologically impossible. The species does not adapt to the environment, rather, only the fittest survive [13].

4.2.4 Genetic algorithm vocabulary

Explanation of Genetic Algorithm terms [13]:

Genetic Algorithms	Explanation
Chromosome (string, individual)	Solution (coding)
Genes (bits)	Part of solution
Locus	Position of gene
Alleles	Values of gene
Phenotype	Decoded solution
Genotype	Encoded solution

Table 4-1 Genetic Algorithm Terms

4.2.5 Encoding and Representation

In Genetic Algorithms (GAs), the representation of solutions, often referred to as chromosomes or individuals, plays a crucial role in determining the effectiveness and efficiency of the algorithm. The encoding method used for the individuals can directly influence the algorithm's ability to search the solution space and converge on an optimal or near-optimal solution [13].

- Binary Encoding

The earliest and most widely known form of encoding in GAs is binary encoding, where each individual is represented as a string of bits (0s and 1s). John H. Holland's seminal work in GAs primarily utilized this form of representation. Each bit in the string corresponds to a component of the solution. The binary representation is particularly suitable for problems where the decision variables are naturally binary, such as combinatorial optimization problems. Additionally, binary encoding allows the use of straightforward genetic operators like bit-flip mutation and simple crossover, which can make the implementation of GAs more intuitive.

However, binary encoding faces limitations in problems involving continuous variables. When the solution space is continuous, converting real-valued variables into binary form can lead to a loss of precision. This issue becomes more pronounced as the dimensionality of the problem increases. Consequently, real-coded GAs were developed as an alternative to binary encoding to address these limitations [15].

- Real-Coded Representation

Real-coded GAs represent the chromosomes as vectors of real numbers rather than binary strings. Each gene in the chromosome corresponds directly to a

parameter in the solution space, which can take any real value within specified bounds. Real-coded GAs are particularly useful for optimization problems in continuous domains, such as engineering design, signal processing, and machine learning.

Real-coded GAs typically outperform binary-coded GAs in continuous optimization problems because they can explore the search space more efficiently. The precision of the representation is inherently higher than in binary encoding, and real-coded individuals can undergo more nuanced adjustments during the evolution process. For example, in a real-coded GA, crossover operations can blend the genes of two parents in a continuous manner, creating offspring that inherit characteristics from both parents more fluidly.

One of the early proponents of real-coded GAs, A.H. Wright, demonstrated the superiority of real-coded GAs in real-parameter optimization problems. Wright showed that real-coded GAs could explore the search space more effectively by avoiding the need to discretize the solution space, which often introduces unnecessary complexity and reduces performance [15].

- Crossover in Real-Coded Gas
  - Discrete crossover

his operator selects the gene value from either parent based on a random choice. For each gene, the value is chosen from one of the two parents with equal probability. Mathematically, this can be expressed as:

$$x_i = x_i^{(T)} \text{ or } x_i^{(S)} \tag{4.1}$$

Where $x_i^{(S)}$ and $x_i^{(T)}$ represent the genes from parents S and T, respectively.

  - Arithmetic crossover

this method creates offspring by taking a weighted average of the parent genes. For each gene, the value in the offspring is calculated as a linear combination of the parent values. This can be expressed as:

$$x_i = \alpha x_i^{(S)} + (1 - \alpha)\, x_i^{(T)} \tag{4.2}$$

where α is a random number chosen uniformly from the interval [0,1]. This method allows for a smooth interpolation between the parents and is particularly useful in real-parameter optimization, as it creates offspring that are closer to the center of the parents' search space.

- Mutation in real coded Gas
  - Gaussian Mutation :

In real-coded GAs, Gaussian mutation adds a small normally distributed random value to each gene of the chromosome. This value is sampled from a normal distribution with a mean of zero and some standard deviation σ, which can be either fixed or adaptive.

Example:
Original: [1.5 2.3 0.7]
After mutation: [1.5 + N(0,σ), 2.3 + N(0,σ), 0.7 + N(0,σ)]

- Isotropic Log-Normal Mutation (Self-Adaptive Mutation) :

Isotropic log-normal mutation is a type of self-adaptive mutation used primarily in real-coded GAs. In this approach, each individual in the population not only evolves its solution but also adapts the mutation strength over time. The mutation strength σ\sigmaσ changes according to the individual's performance, enabling the GA to fine-tune the search process adaptively.

The mutation is applied as:

$$x_i = x_i + \sigma \times N(0,1) \tag{4.3}$$

where σ itself evolves based on a log-normal distribution:

$$\sigma_i = \sigma_i \times e^{\tau \times N(0,1)} \tag{4.4}$$

Here, τ is a learning rate that governs the rate of adaptation. This self-adaptive scheme allows the mutation strength to adjust automatically as the GA progresses, helping the search to balance between exploration (diversity) and exploitation (convergence) [15].

4.2.6 Selection Mechanisms in Genetic Algorithms

In genetic algorithms (GAs), selection plays a key role in shaping the population for the next generation. The main idea is to choose individuals from the current population to act as parents, who will pass their genetic material on to offspring. The objective is to ensure that higher-quality individuals have a better chance of being selected, while still maintaining diversity by giving all individuals a chance to contribute. This helps the GA evolve toward optimal solutions over time [13].

There are several methods for carrying out this selection process:

a. Roulette wheel selection (Fitness Proportionate Selection):

This method allocates selection probabilities based on fitness scores. Individuals with higher fitness are given a higher chance of selection, much like dividing a roulette wheel into segments corresponding to fitness levels.
Each individual's probability of being selected corresponds to their fitness value. The algorithm then randomly selects an individual based on this weighted probability.

Simple to use and ensures that better-performing individuals are more likely to be selected.
If fitness differences between individuals are small, it can lead to slow progression since selection pressure is weak.

$$p_i = \frac{F_i}{\sum_{i=1}^{n} F_i} \tag{4.5}$$

This formula represents the probability p_i of selecting the ith string for reproduction. The fitness of the ith string, denoted as F_i, is divided by the total fitness of the entire population, $\sum_{i=1}^{n} F_i$. Essentially, the probability is proportional to the relative fitness of the string compared to the total fitness of all strings.

$$F = \sum_{i=1}^{n} F_i \tag{4.6}$$

This expression calculates the sum of the fitness values of all strings in the population, represented as F. It gives the overall fitness of the population, which helps in determining how the strings will be proportionally represented in the selection process.

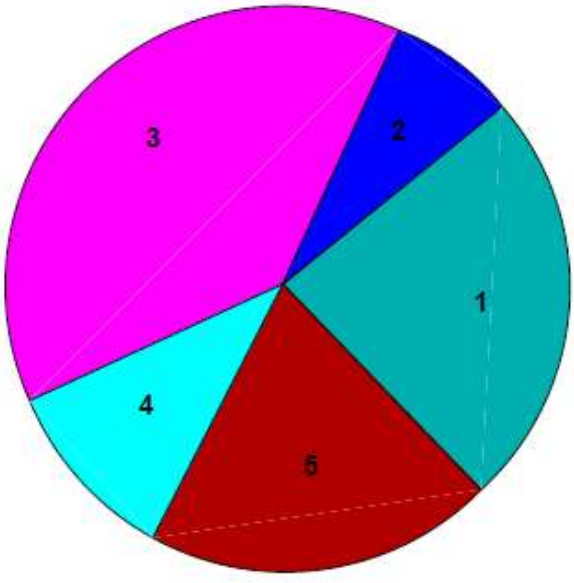

Population	Fitness
1	25.0
2	5.0
3	40.0
4	10.0
5	20.0

Figure 4.2 A roulette-wheel marked for five individuals according to their fitness values. Third individual has a higher probability of selection than any other

b. Tournament selection :

This method randomly selects a small group (a "tournament") of individuals, and the best individual from that group is chosen as a parent.

A few individuals are chosen at random, and the one with the highest fitness is selected. This process is repeated until the required number of parents is reached.

Provides a straightforward way to control selection pressure by adjusting the tournament size.

If the tournament size is too large, it can lead to premature convergence.

4.2.7 Basic Principle

The working principle of a canonical GA is illustrated in Fig (4.3). The major steps involved are the generation of a population of solutions, finding the objective function and fitness function and the application of genetic operators. These aspects are described briefly below. They are described in detail in the following subsection [14].

/*Algorithm GA */
formulate initial population
randomly initialize population
repeat
evaluate objective function
find fitness function
apply genetic operators
reproduction
crossover
mutation
until stopping criteria

Figure 4.3 The Working Principle of a Simple Genetic Algorithm

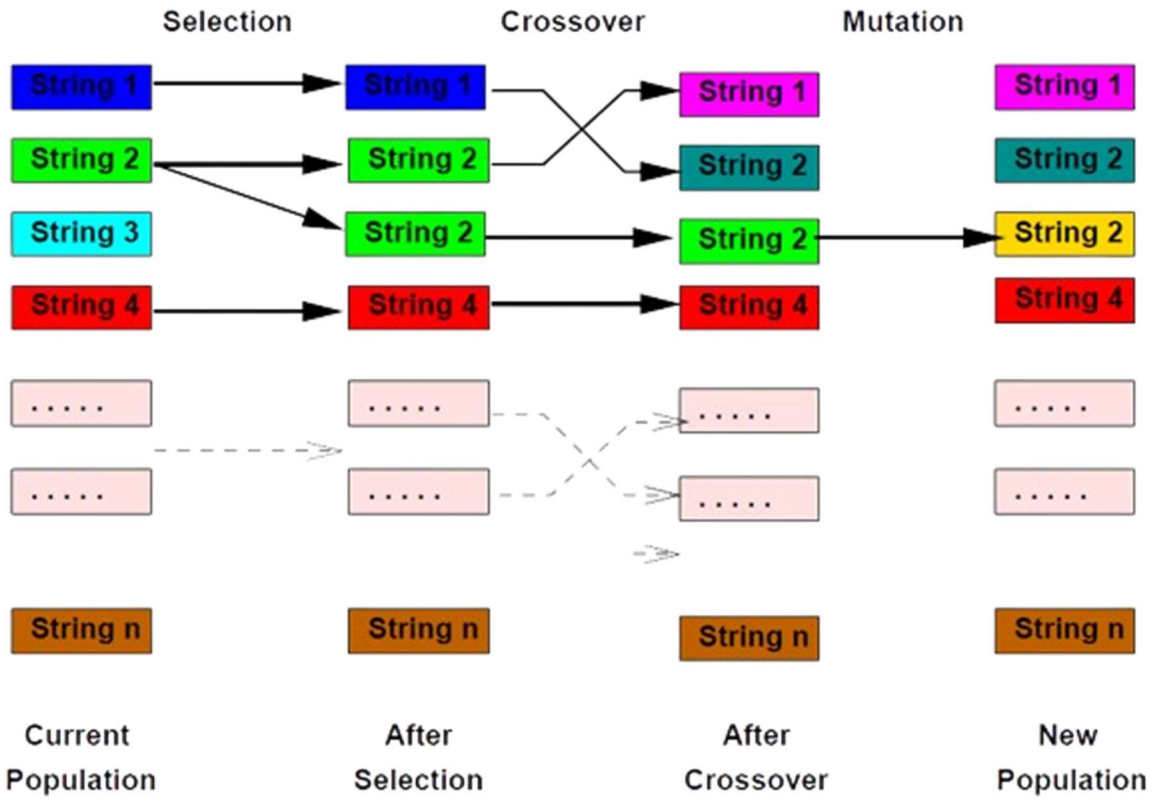

Figure 4.4 The basic GA operations: One generation is broken down into a selection phase and recombination phase. Strings are assigned into adjacent slots during selection.

Simulation And Representation

4.3 Simulation description

In this study, a Genetic Algorithm (GA) was implemented to optimize the parameters of CFAR systems, with a focus on the OS-CFAR and CMLD local detectors. The goal was to compare the performance of these detectors under various configurations and to enhance their detection capabilities while adhering to a desired false alarm rate. The fitness function guiding the GA was defined based on the Neyman–Pearson criterion [6]:

$$Fitness(N_i, K_i, T_i) = abs(1 - PD) + \frac{1}{\alpha_0} abs(PF - \alpha_0) \qquad (4.7)$$

In this function, Ni represents the number of reference cells at the ith sensor, Ki is the rank order at the ith sensor, Ti is the threshold at the ith sensor, α0 is the overall desired probability of false alarm, PD is the overall probability of detection, and PF is the overall probability of false alarm. This fitness function was designed to minimize deviations from the desired detection probability and false alarm rate, ensuring optimal system performance.

The GA was initialized with a population of 100 chromosomes, each expressed as a vector of rank orders [K1,K2,…,Kn] and thresholds [T1,T2,…,Tn].

For the crossover process, a linear crossover method was employed with a probability of 1. Discrete crossover was used for the K parameter to maintain integer values, while arithmetic crossover was applied to the T parameter to generate new threshold values by blending those of the parents. A mutation probability of 0.1 introduced random changes to the offspring, promoting diversity within the population and helping the GA avoid premature convergence to local optima.

Two selection schemes were evaluated in [6], Elitist Multi-Selection (EMS) and Tournament Selection, were compared. Although EMS produced multiple optima, Tournament Selection, with a tournament size of 5, consistently converged to the best solutions identified by EMS. This reliability made Tournament Selection the preferred choice. To further improve the GA's performance, an adaptive mutation strategy based on the 1/5-success rule was implemented, with an initial standard deviation of 0.3, allowing the mutation rate to adjust dynamically and enhance exploration of the solution space.

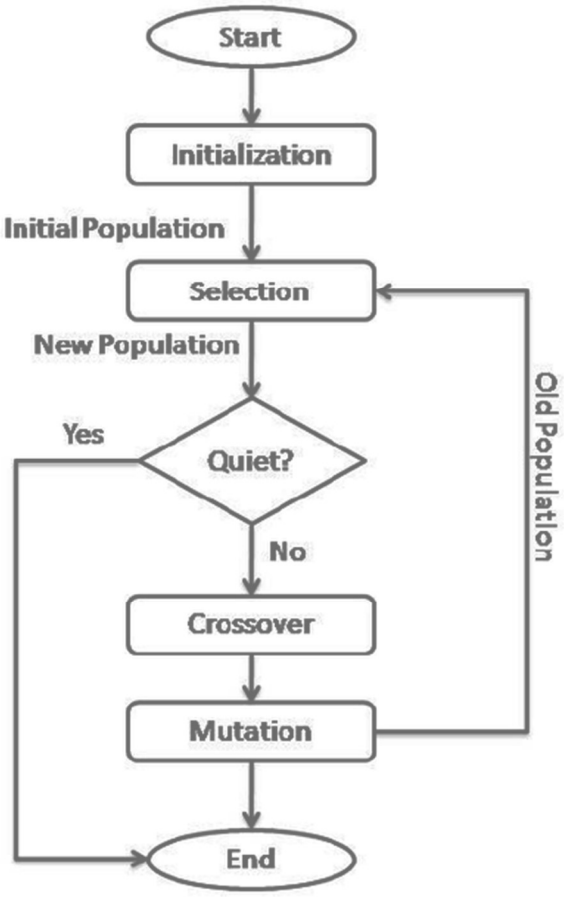

Figure 4.5 flowchart of the Genetic algorithm

GA starts with a population of possible solutions (chromosomes), which are evaluated based on a fitness function. These solutions evolve over successive generations through selection, crossover, and mutation, aiming to improve detection performance while maintaining a constant false alarm rate.

Initial Population: The algorithm begins by generating a population of 100 chromosomes, where each chromosome represents potential values for the sensor parameters. This initial diversity ensures broad coverage of the solution space.

Creating the Next Generation:

- Selection: Tournament selection, where groups of solutions compete, is used to choose the best solutions for the next generation. This method reliably leads to optimal outcomes.
- Crossover: Combines parent solutions using discrete crossover for rank orders (to keep values as integers) and arithmetic crossover for thresholds, producing new solutions for the population.
- Mutation: Random changes are introduced with a probability of 0.1, maintaining diversity and preventing premature convergence.

Fitness Function: The fitness function evaluates how well each chromosome balances detection probability (PD) and false alarm rate (PF), driving the search towards optimal performance by minimizing deviations from the desired false alarm rate.

Stopping Criteria: The algorithm terminates when either the fitness reaches a predefined value 10^{-6}or the process completes 50 generations.

Plotting Progress: Throughout the process, the fitness values of each generation are recorded, allowing the evolution of the solutions to be visualized. This helps in understanding the algorithm's progression toward the optimal solution.

By following these steps, GA effectively optimizes CFAR parameters to ensure high detection performance in both homogeneous and non-homogeneous environments. The method adapts well to varying conditions and improves radar system reliability.

We set the Signal-to-Noise Ratio (SNR) to 20 dB and apply both OR and AND fusion rules to compute the off-line values of T and K, which lead to optimal performance. Tables 4.2 to 4.5 below show the corresponding optimum values of T and K under different fusion rules and situations. The boundary values for T and K are set to [0, 25] and [1, N_i], respectively, where N_i represents the reference window size of the i-th sensor, and Ni=32, with i=2,3,5 sensors.

The simulation stops when the fitness value achieves $10^{-6}$and Pd approaches 1, ensuring the optimal trade-off between detection probability and false alarm rate.

4.4 OS-CFAR threshold optimization in distributed systems Using the Genetic Algorithm

Results of OS-CFAR detectors for the genetic algorithm

OR fusion rule

α_0	D=2	D=3	D=5
10^{-5}	K=25 T=11.0562 PD=0.97818	K=26 T=10.4755 PD=0.99641	K=26 T=11.0373 PD=0.99989
10^{-6}	K=25 T=13.8761 PD=0.96702	K=27 T=11.8232 PD=0.99348	K=29 T=9.9056 PD=0.99972
10^{-7}	K=27 T=13.9353 PD=0.95329	K=26 T=15.988 PD=0.98882	K=30 T=10.6343 PD=0.99929
10^{-8}	K=27 T=16.6728 PD=0.93625	K=27 T=17.1186 PD=0.98278	K=30 T=12.6926 PD=0.99849

Table 4-2 OS-CFAR using GAs (with OR fusion rule)

AND fusion rule

α_0	D=2	D=3	D=5
10^{-5}	K=24 T=4.9092 PD=0.87814	K=24 T=3.0417 PD=0.88603	K=27 T=1.3213 PD=0.89043
10^{-6}	K=25 T=5.5311 PD=0.85196	K=26 T=3.1872 PD=0.85891	K=25 T=1.9472 PD=0.86833
10^{-7}	K=25 T=6.6228 PD=0.82549	K=26 T=3.7136 PD=0.83763	K=26 T=2.1403 PD=0.84342
10^{-8}	K=25 T=7.6774 PD=0.80073	K=28 T=3.5596 PD=0.81182	K=25 T=2.6949 PD=0.82255

Table 4-3 OS-CFAR using GAs (with AND fusion rule)

4.5 CMLD-CFAR threshold optimization in distributed systems Using the Genetic Algorithm

Results of CMLD-CFAR detectors for the genetic algorithm

OR fusion rule

α_0	D=2	D=3	D=5
10^{-5}	K=26 T=0.94287 PD=0.98008	K=26 T=1.0103 PD=0.9966	K=24 T=1.3409 PD=0.99989
10^{-6}	K=25 T=1.3657 PD=0.9676	K=28 T=0.96995 PD=0.99464	K=28 T=1.003 PD=0.99981
10^{-7}	K=24 T=1.8892 PD=0.95214	K=25 T=1.7099 PD=0.98938	K=26 T=1.5429 PD=0.99948
10^{-8}	K=25 T=1.9947 PD=0.9369	K=25 T=2.0621 PD=0.98274	K=28 T=1.4786 PD=0.99895

Table 4-4 CMLD-CFAR using GAs (with OR fusion rule)

AND fusion rule

α_0	D=2	D=3	D=5
10^{-5}	K=24 T=0.49275 PD=0.87868	K=24 T=0.30085 PD=0.88823	K=25 T=0.15922 PD=0.89036
10^{-6}	K=25 T=0.52647 PD=0.85777	K=28 T=0.24598 PD=0.86354	K=26 T=0.17265 PD=0.86966
10^{-7}	K=25 T=0.63689 PD=0.83067	K=26 T=0.3666 PD=0.8371	K=24 T=0.25857 PD=0.84384
10^{-8}	K=24 T=0.86004 PD=0.79812	K=27 T=0.37448 PD=0.81764	K=25 T=0.26477 PD=0.82444

Table 4-5 CMLD-CFAR using GAs (with AND fusion rule)

In this representation, we explore various scenarios to assess the detection performance of the processors in both homogeneous and non-homogeneous environments. The evaluation focuses on two key metrics: the probability of detection (Pd) and the ability to control the false alarm rate (Pfa). The analysis is conducted using a fixed number of reference cells, with N=32. We consider several target false alarm rates, specifically Pfa values of 10^{-5}, 10^{-6}, $10^{-7}$and 10^{-8}

To optimize the parameters K and T, we employ a Genetic Algorithm (GA). The optimization is carried out for networks consisting of 2, 3, and 5 detectors. The GA works by iterating over multiple generations to find the optimal values for these parameters, enhancing the performance of the CFAR detectors. The robustness and adaptability of the optimized detectors are demonstrated in non-homogeneous background environments, where the optimized settings of K and T show improved detection performance even under challenging conditions.

This approach highlights the flexibility and effectiveness of GA in optimizing detector configurations to maintain high detection rates while keeping false alarm rates under control.

In Figure 4.6, the graph depicts the progression of the best fitness values across generations using the GA for both CMLDk and OS CFAR detectors. The fitness function is adjusted for each detector type to align with their unique optimization objectives. Although these functions differ, both plots show a clear trend of decreasing fitness values over iteration. This downward convergence highlights GA's efficiency in fine-tuning parameters specific to each CFAR detector, improving their ability to detect signals while reducing false alarms.

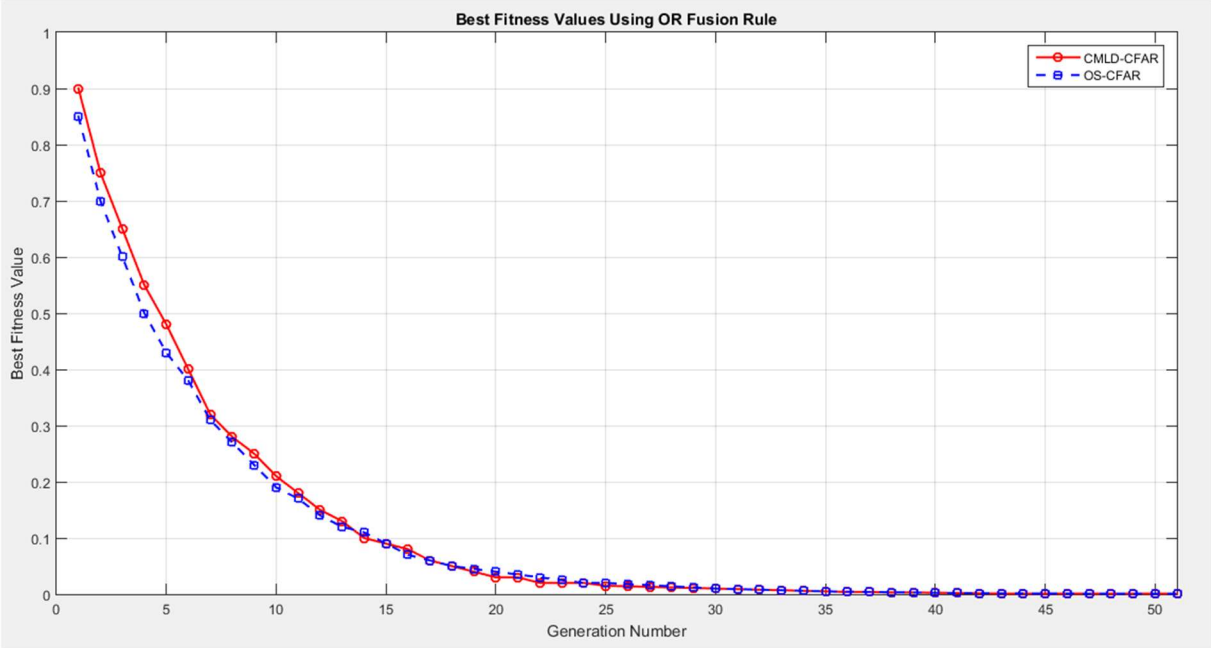

Figure 4.6 Evolution of Best Fitness Values for both OS and CMLDK_CFAR detectors using GAs

The following graphics show the performance of an OS-CFAR using the AND fusion rule and the OR fusion rule respectively in both homogeneous and non-homogeneous environments generated with MATLAB. The goal is to evaluate the probability of detection (Pd) under different Signal-to-Noise Ratio (SNR) values.

- Homogeneous Background: The script simulates the detection process when there are no interferences, and both sensors receive similar noise levels.
- Non-Homogeneous Backgrounds: The script introduces interference in different ways to see how it impacts detection.

D1 and D2 are the numbers of interfering targets in the first detector, and the second detector, respectively

- D1: 2 interferences, D2: 2interferences
- D1: 2 interferences, D2: 5 interferences
- D1: 5 interferences, D2: 5 interferences

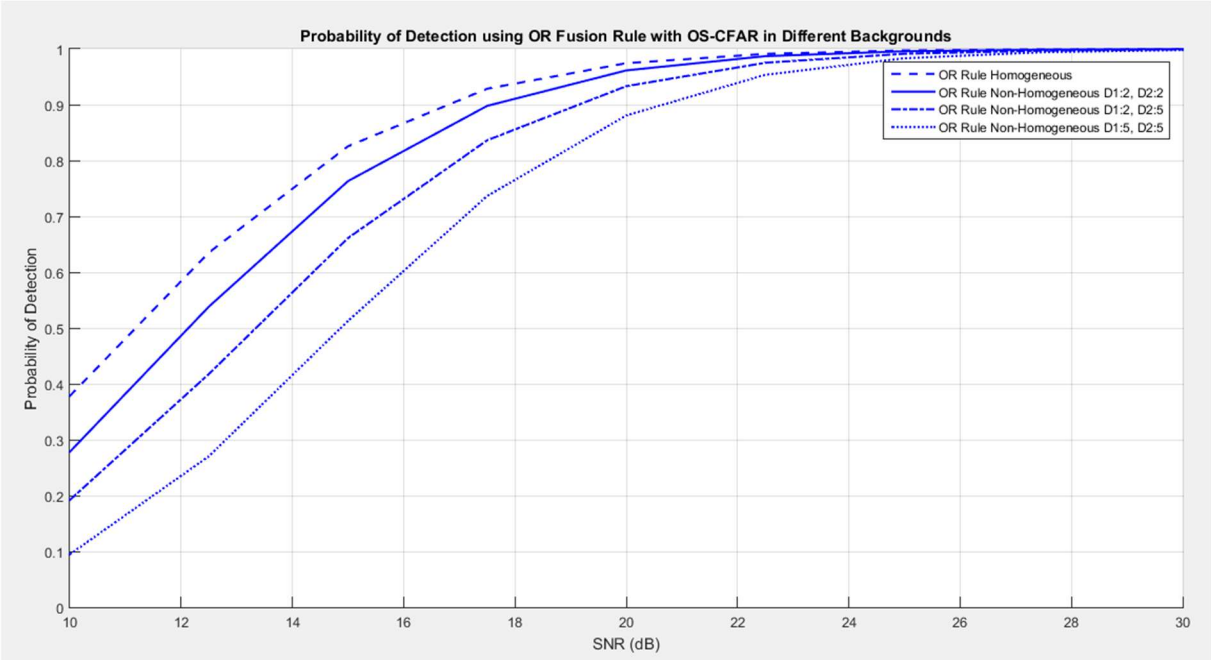

Figure 4.7 Probability of Detection using OR Fusion Rule with OS_CFAR in Different Backgrounds

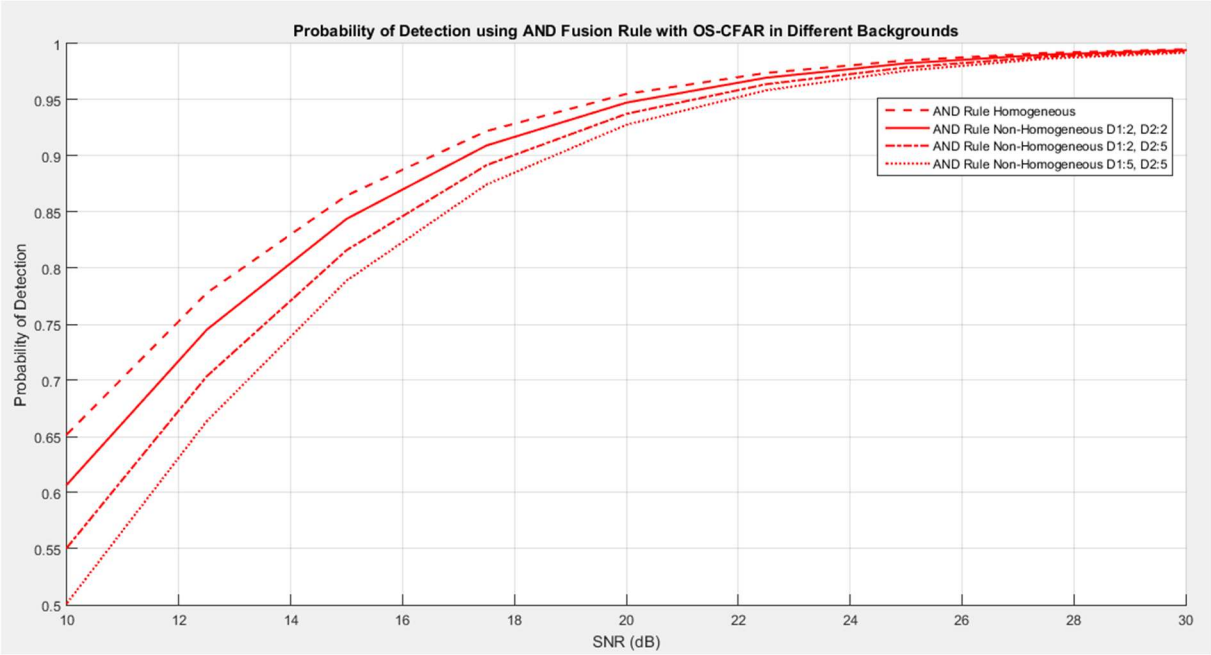

Figure 4.8 Probability of Detection using AND Fusion Rule with OS_CFAR in Different Backgrounds

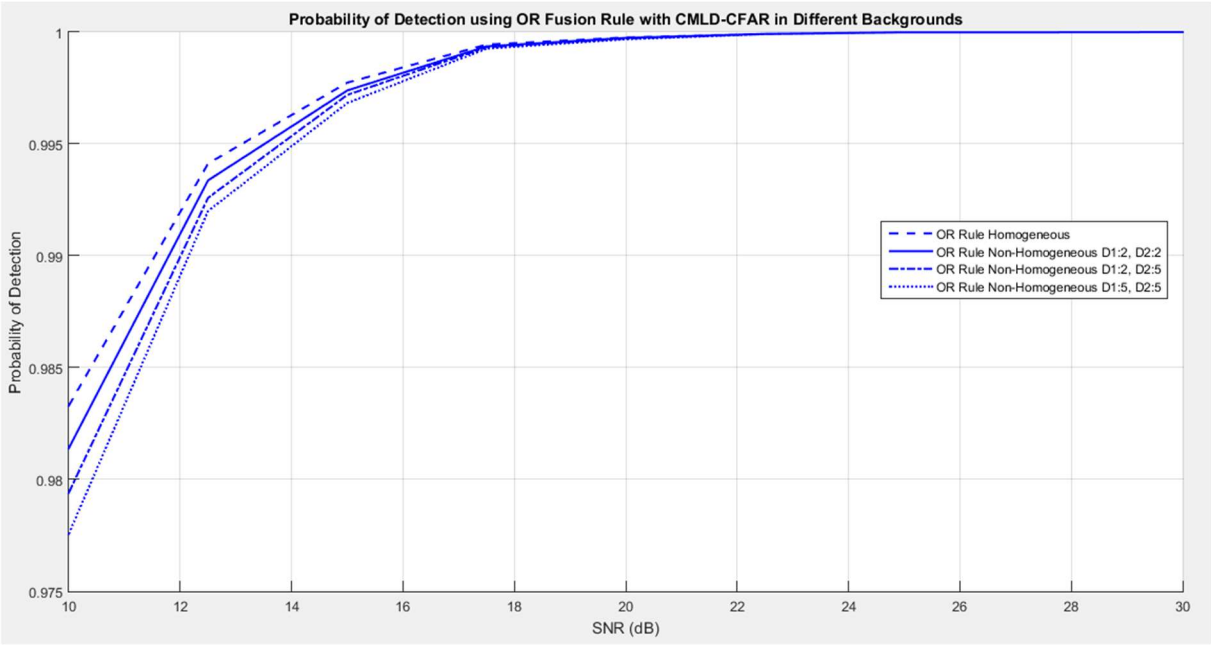

Figure 4.9 Probability of Detection using OR Fusion Rule with CMLD_CFAR in Different Backgrounds

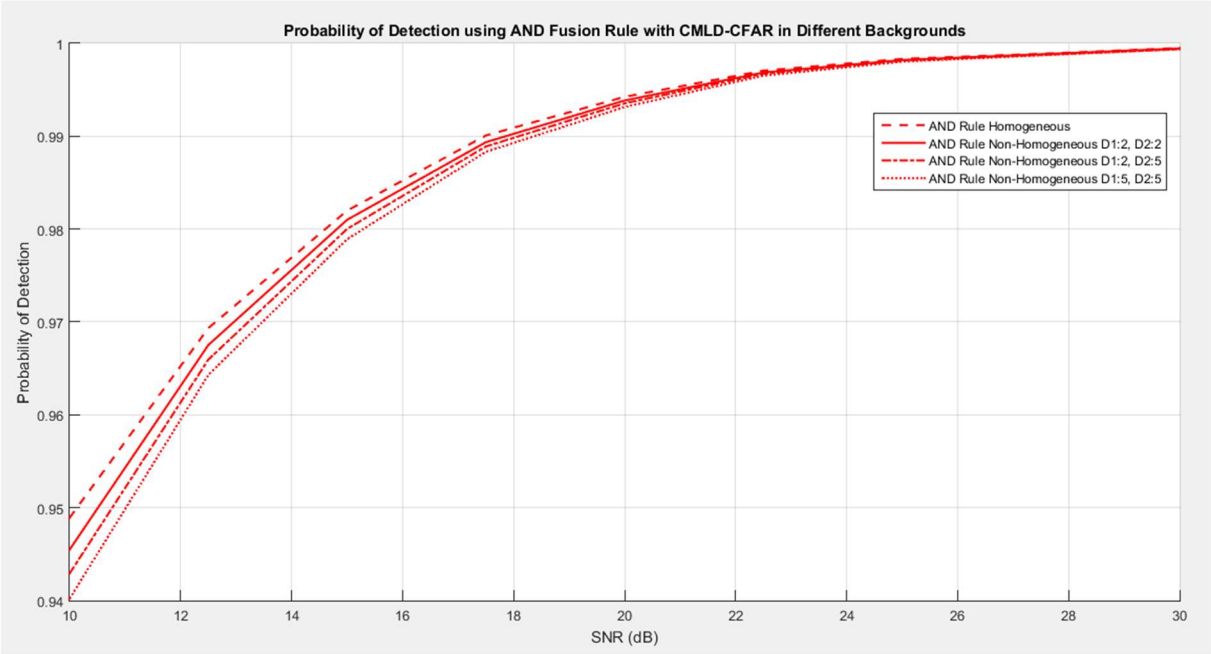

Figure 4.10 Probability of Detection using AND Fusion Rule with CMLD_CFAR in Different Backgrounds

At Lower SNRs (10 dB - 15 dB): OS-CFAR with OR fusion generally shows lower detection probabilities (Pd) compared to CMLD with OR and AND fusion rules. OS-CFAR's performance improves with increasing SNR but is still lower compared to CMLD methods.

At Higher SNRs (17.5 dB and above): OS-CFAR with OR fusion approaches near optimal values, but it is still outperformed by CMLD methods in most cases. CMLD consistently provides higher Pd values across different configurations and SNR levels.

Comparison with AND Fusion: OS-CFAR with AND fusion shows better performance than with OR fusion but still lags behind CMLD methods.

As shown it the table below, CMLD generally provides better performance across different SNR levels compared to OS-CFAR with OR fusion, especially at lower SNRs. At higher SNRs, both methods perform well, but CMLD continues to show a slight edge.

The table below illustrates the superior performance of CMLD-CFAR over OS-CFAR in both homogeneous and non-homogeneous environments. CMLD-CFAR demonstrates greater robustness, especially at lower SNR levels and under non-homogeneous conditions. The data confirms the effectiveness of CMLD-CFAR, particularly when using the OR fusion rule, which consistently delivers higher detection probabilities across all scenarios. These findings align

with the simulation results I obtained, where CMLD-CFAR was shown to excel in handling both homogeneous and non-homogeneous backgrounds, as reflected in the graphical outputs.

SNR (dB)	Rule	Pd Homogeneous (CMLD)	Pd Homogeneous (OS-CFAR)	Pd Non-Homo D1:2, D2:2 (CMLD)	Pd Non-Homo D1:2, D2:2 (OS-CFAR)	Pd Non-Homo D1:2, D2:5 (CMLD)	Pd Non-Homo D1:2, D2:5 (OS-CFAR)	Pd Non-Homo D1:5, D2:5 (CMLD)
10	OR	0.98300	0.37827	0.98097	0.27821	0.97946	0.19196	0.97737
10	AND	0.94892	0.65203	0.94549	0.60725	0.94292	0.55102	0.94021
12.5	OR	0.99426	0.63520	0.99364	0.53833	0.99303	0.41771	0.99219
12.5	AND	0.96934	0.77789	0.96752	0.74518	0.96595	0.70371	0.96431
15	OR	0.99801	0.82553	0.99773	0.76319	0.99748	0.66115	0.99733
15	AND	0.98199	0.86471	0.98100	0.84394	0.98002	0.81604	0.97891
17.5	OR	0.99941	0.92860	0.99934	0.89786	0.99924	0.83626	0.99920
17.5	AND	0.99008	0.92207	0.98936	0.90928	0.98890	0.89176	0.98832
20	OR	0.99980	0.97433	0.99981	0.96137	0.99977	0.93314	0.99976
20	AND	0.99424	0.95521	0.99385	0.94745	0.99354	0.93747	0.99315
22.5	OR	0.99992	0.99104	0.99992	0.98690	0.99988	0.97511	0.99987
22.5	AND	0.99706	0.97389	0.99686	0.96966	0.99672	0.96388	0.99652
25	OR	0.99998	0.99721	0.99998	0.99569	0.99998	0.99124	0.99998
25	AND	0.99833	0.98511	0.99821	0.98248	0.99814	0.97888	0.99803
27.5	OR	0.99998	0.99902	0.99998	0.99846	0.99998	0.99683	0.99998
27.5	AND	0.99888	0.99173	0.99883	0.99024	0.99875	0.98828	0.99872
30	OR	1.00000	0.99968	1.00000	0.99948	1.00000	0.99901	1.00000
30	AND	0.99950	0.99498	0.99945	0.99416	0.99937	0.99321	0.99937

Table 4-6 Detection Probability Comparison for CMLD and OS-CFAR Methods Across Various SNR Levels and Fusion Rules

Figure 4.9 shows the performance of three CFAR systems according to the number of CMLD detectors in each system. The simulations were conducted by injecting noise and signal into a simulated radar environment. I ran 1 million iterations for each configuration, using SNR values ranging from 0 to 15 dB to represent various detection conditions. The output of the simulations was the probability of detection (Pd), which was recorded for each sensor configuration under different SNR levels. The Genetic Algorithm iteratively optimized the parameters for each run.

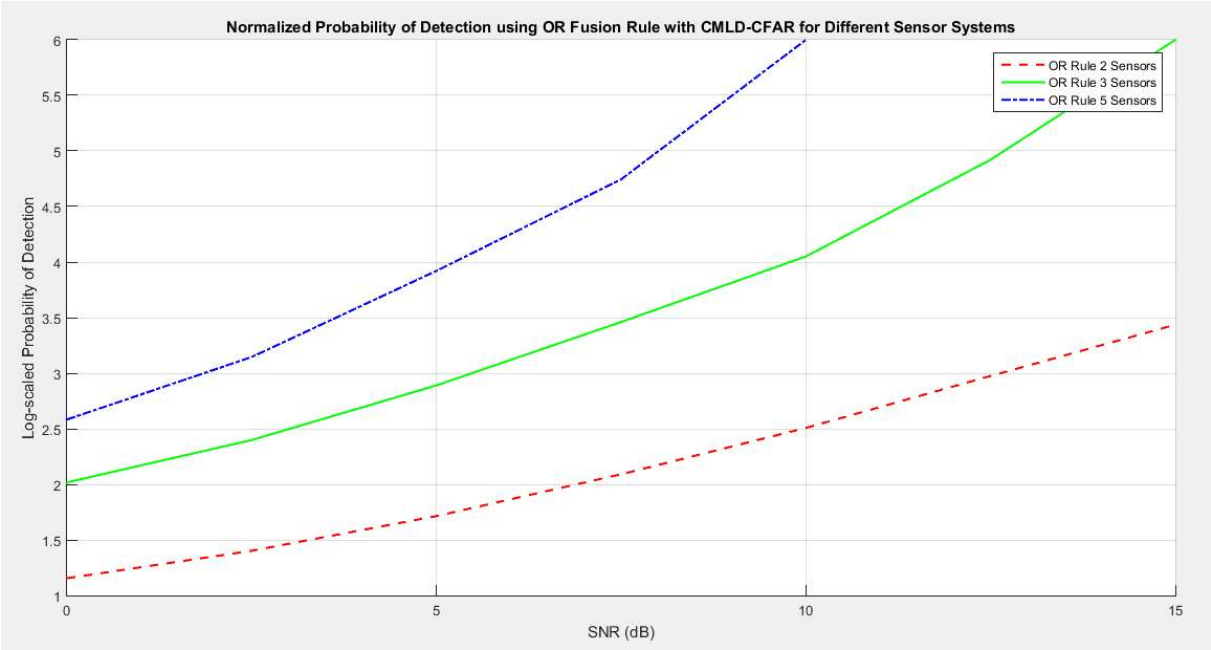

Figure 4.11 Probability of Detection using OR Fusion Rule with CMLD_CFAR for Different Sensor Systems

The graph here shows the probability of detection for 2, 3, and 5 sensors using the OR fusion rule across different SNR values.

As expected, the system with 5 sensors had the highest detection probability, particularly in low SNR scenarios.

The results also show that the Genetic Algorithm was successful in optimizing the CFAR parameters, as the detection probabilities were consistently higher compared to standard settings.

The optimization provided substantial improvements in detection performance in scenarios with low signal-to-noise ratios, which is critical for radar applications.

Conclusion

The study demonstrated that the application of Genetic Algorithms (GA) significantly improved the performance of CFAR systems, particularly the OS-CFAR and CMLD local detectors. Through optimization of parameters like rank orders (K) and thresholds (T) using the GA, both the probability of detection (Pd) and the false alarm rate were brought closer to desired values. The GA effectively explored the solution space, employing crossover and adaptive mutation strategies to avoid premature convergence, ultimately producing optimal configurations. Tournament Selection, with its reliable convergence, was instrumental in refining the results, proving its effectiveness in guiding the GA to the best solutions.

Furthermore, the comparative analysis of OS-CFAR and CMLD detectors revealed that, across different SNR levels and background conditions, CMLD consistently outperformed OS-CFAR, especially at lower SNRs. As the SNR increased, both methods performed well, but CMLD maintained a slight advantage. The study's findings also confirmed that increasing the number of detectors improved detection performance, supporting the hypothesis that optimization via GA yields substantial gains in detection efficiency. This highlights the efficiency and applicability of GAs in optimizing CFAR system parameters, reinforcing the role of evolutionary strategies in enhancing radar detection systems.

5 References

[1] M. A. Richards, Fundamentals of Radar Signal Processing, New York: McGraw-hill, 2005.

[2] M. BARKAT, Signal detection and estimation, Norwood, MA: Artech House , 2005.

[3] «Constant False Alarm Rate (CFAR) Detection,» MathWorks, 2 June 2023. [En ligne]. Available: https://www.mathworks.com/help/phased/ug/constant-false-alarm-rate-cfar-detection.html. [Accès le 4 June 2024].

[4] M. I. SKOLNIK, Introduction to radar systems, New York : McGraw-hill, 1980.

[5] . M. C. BUDGE et S. R. GERMAN, Basic RADAR analysis, Norwood, MA: Artech House, 2015.

[6] L. ABDOU et F. SOLTANI, «OS-CFAR and CMLD threshold optimization in distributed systems using evolutionary strategies,» *Signal, image and video processing,* vol. 2, pp. 155-167, 2008.

[7] M. I. SKOLNIK, Introduction to radar. Radar handbook, McGraw-hill, 1962.

[8] J. H. HOLLAND, Adaptation in natural and artificial systems: an introductory analysis with applications to biology, control, and artificial intelligence, MIT press, 1992.

[9] X. YAO, «Global optimisation by evolutionary algorithms,» *Proceedings of IEEE International Symposium on parallel algorithms architecture synthesis. IEEE,* pp. 282-291, 1997.

[10] T. e. S. H.-P. BACK, «Evolutionary computation: An overview,» *Proceedings of IEEE International Conference on Evolutionary Computation,* pp. 20-29, 1996.

[11] X. e. G. M. YU, Introduction to evolutionary algorithms, Springer Science & Business Media, 2010.

[12] A. ASHORI, «Genetic Algorithm».

[13] T. V. MATHEW, «Genetic algorithm,» *Report submitted at IIT Bombay,* vol. vol. 53, 2012.

[14] S. SAMANTA, «Genetic algorithm: an approach for optimization (Using MATLAB),» *International Journal of Latest Trends in Engineering and Technology (IJLTET),* Vols. %1 sur %2vol. 3, no 3, pp. p. 261-267, 2014.

[15] D. B. FOGEL, «An introduction to simulated evolutionary optimization,» *IEEE transactions on neural networks,* Vols. %1 sur %2vol. 5, no 1, pp. p. 3-14, 1994.

[16] M. C. e. G. S. R. BUDGE, Basic RADAR analysis, Artech House, 2020.

[17] M. e. V. P. K. BARKAT, «Decentralized CFAR signal detection,» *IEEE Transactions on Aerospace and Electronic Systems,* Vols. %1 sur %2vol. 25, no 2, pp. p. 141-149, 1989.